



Alginate-based diblock polymers: preparation, characterization and Ca-induced self-assembly

Amalie Solberg, Ingrid V. Mo, Finn L. Aachmann, Christophe Schatz, Bjørn E. Christensen

► To cite this version:

Amalie Solberg, Ingrid V. Mo, Finn L. Aachmann, Christophe Schatz, Bjørn E. Christensen. Alginate-based diblock polymers: preparation, characterization and Ca-induced self-assembly. *Polymer Chemistry*, 2021, 12 (38), pp.5412-5425. <10.1039/d1py00727k>. <hal-03511278>

HAL Id: hal-03511278

<https://hal.science/hal-03511278v1>

Submitted on 4 Jan 2022

HAL is a multi-disciplinary open access archive for the deposit and dissemination of scientific research documents, whether they are published or not. The documents may come from teaching and research institutions in France or abroad, or from public or private research centers.

L'archive ouverte pluridisciplinaire **HAL**, est destinée au dépôt et à la diffusion de documents scientifiques de niveau recherche, publiés ou non, émanant des établissements d'enseignement et de recherche français ou étrangers, des laboratoires publics ou privés.



Distributed under a Creative Commons CC BY-NC-SA 4.0 - Attribution - Non-commercial use - ShareAlike - International License

Alginate-based diblock polymers: Preparation, characterization and Ca-induced self-assembly[†]

Amalie Solberg,^a Ingrid V. Mo,^a Finn L. Aachmann,^a Christophe Schatz^{*b} and Bjørn E. Christensen^{*a}

Renewable resources can provide a range of different polysaccharide blocks that can be used to prepare new types of stimuli-responsive polysaccharide-based block copolymers. Alginates are natural polysaccharides widely used as biomaterials. Functional properties depend on the content and distribution of the two 4-linked monomers (β -D-mannuronate (M) and α -L-guluronate (G)). Blocks of L-guluronate (G_n), are responsible for cooperative binding of calcium ions and hydrogel formation. Incorporation of such blocks in block polysaccharide copolymers would represent a new class of engineered, Ca-sensitive biomacromolecules. Dioxyamines and dihydrazides have recently been shown to be well suited for preparation of block polysaccharides structures. Here we first show that when applied to alginate blocks (G_n and M_n) the two types are both very reactive, but the detailed distribution

^a NOBIPOL, Department of Biotechnology and Food Science, NTNU Norwegian University of Science and Technology, Sem Sælands vei 6/8, NO-7491 Trondheim, Norway

^b LCPO, Université de Bordeaux, UMR 5629, ENSCBP, 16, Avenue Pey Berland, 33607 Pessac Cedex, France

[†] Electronic supplementary information (ESI) available: Time course NMR, characterization of conjugates and kinetic plots for conjugation reactions.

of acyclic (*E*)- and (*Z*)-forms and cyclic N-pyranosides, reaction kinetics, conjugate stability, and the rate of Schiff base reduction with α -picoline borane differ considerably, also compared to other polysaccharides. Hence, alginate specific protocols were developed.

The linkers introduce a highly flexible joint in otherwise semiflexible G_n -based diblocks. This was demonstrated by SEC-MALS using a symmetrical G_n -*b*- G_n diblock, which in solution can best be described according to a broken rod model. Ca-induced self-assembly of G_n -*b*-dextran diblocks was studied by dynamic light scattering, demonstrating that well defined nanoparticles could be prepared for certain combinations of chain lengths. Taken together, this approach provides a new class of engineered, stimuli-responsive block polysaccharide copolymers solely based on natural resources.

Introduction

Alginates are linear, anionic polysaccharides of 4-linked β -D-mannuronic acid (M) and its C5-epimer, 4-linked α -L-guluronic acid (G) (Fig. 1). They are produced by brown algae, some red algae, as well as some bacterial species.^{1, 2} Alginates have found numerous application areas in foods, biomaterials and pharmaceuticals due to their mild gelation properties in addition to being used as viscosifiers.¹ The monomers are located within homopolymeric M-blocks and G-blocks, as well as alternating (..MG..) blocks. The blocks coexist in alginate chains but in widely different proportions, depending on the source.³ The G-blocks are largely responsible for the gel formation with divalent cations.⁴ Although alginates may themselves be classified as block polysaccharides, the length and distribution of the three block types vary due to the inherent compositional heterogeneity of alginates.¹ The relationship between the gelling properties of alginates with multivalent cations and the structure, sequence and chain length of alginates has been extensively investigated for decades.^{1, 2, 4} In contrast, the properties of

isolated M- and G-blocks and their incorporation in block polysaccharides have only been sporadically studied.

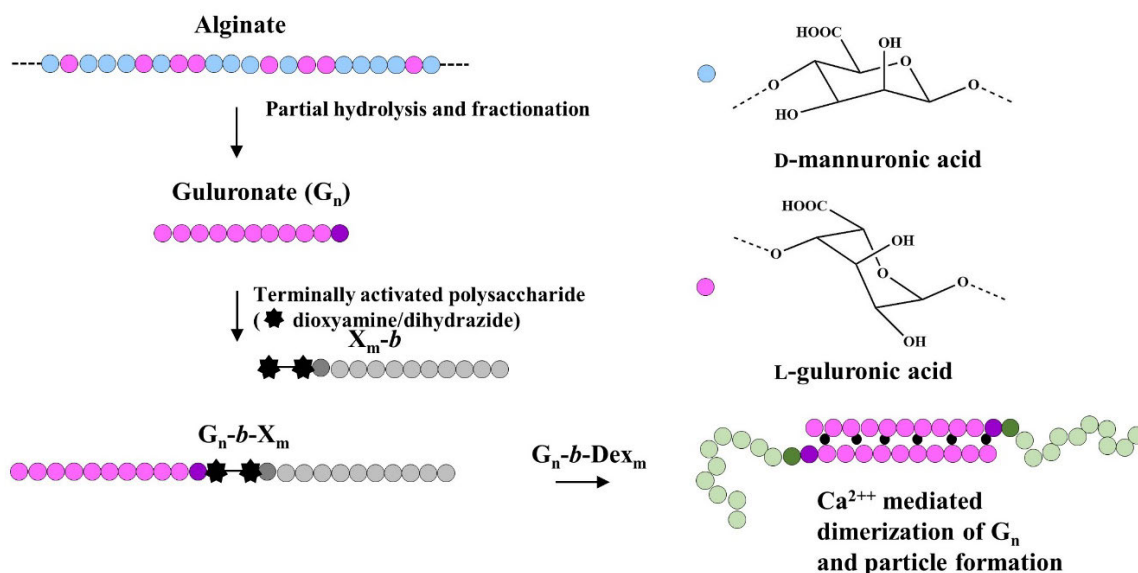


Fig. 1 Preparation of guluronate blocks (G_n) from alginates and their terminal conjugation to an activated polysaccharide, followed by the chain dimerization with Ca^{2+} and G_n -b-Dex_m.

Block polysaccharides consist of two or more oligo- or polysaccharide blocks connected at the chain termini through a suitable conjugation method. One of the main motivations for the study of diblock polysaccharides is to exploit their self-assembly properties under defined conditions. Blocks can be combined such that one block can develop short-range attractive interactions while the other develop long-range repulsive interactions. The resulting self-assembly is a spontaneous process leading to a great diversity of structures whose characteristics depend on the molecular parameters of the individual blocks. In the case of alginates, the strong and specific interactions of G-blocks with Ca^{2+} , Sr^{2+} and Ba^{2+} could be balanced by repulsive interactions with a neutral polysaccharide block such as dextran when linearly conjugated to the G block.

We recently utilised click-like reactions based on a dihydrazide and a dioxyamine^{5, 6} to prepare chitin- and chitosan-based^{7, 8} diblock polysaccharides through conjugation at the reducing end. In the case of polyuronates such as alginates corresponding click reactions are particularly attractive alternatives to the conventional alkyne-azide cycloaddition catalysed by copper because of its strong complexation with polyuronates.⁹ For alginate blocks very little is known about the reactivity at the reducing ends, but it has been demonstrated that an aminoxy-peptide can conjugate to alginates by aniline-catalysed oxime click.⁶

Here we show that both oligoguluronates (G-blocks, G_n) and oligomannuronates (M-blocks, M_n), when compared to e.g. dextran and chitosan, react relatively fast at the reducing end with both PDHA (O,O'-1,3,-propanediylbis(hydroxylamine dihydrochloride) and ADH (adipic acid dihydrazide), with no or low dependence on the chain length. We further study the reactivity of G_n with several PDHA/ADH-activated oligosaccharides and oxyamine-functionalized PEGs. The oxime/hydrazone reduction with PB is also studied. Protocols for effective conjugations are provided. As proof-of-principle we prepare several diblock-polysaccharides based on oligoguluronate. We further demonstrate characteristic solution properties of an oligoguluronate-based diblocks associated with the flexible linker by means of multidetector SEC. Finally, we show that G_n -PDHA-dextran diblocks forms nanoparticles in the presence of Ca^{2+} ion for certain combinations of chain lengths, in contrast to pure oligouronates, which form solid precipitates.

Experimental

Materials

Guluronic acid oligomers (G oligomer) with two different molecular weight distributions were prepared¹⁰ from partially acid hydrolysed, high guluronate alginate from *Laminaria hyperborea* stipes by

acid precipitation to give oligomers with a number average degree of polymerization (DP_n) of 21 and a fraction of guluronic acid (F_G) of 0.90 (determined by NMR). Samples with DP_n of 4 and 10 were prepared by further hydrolysis.

Trimannuronate was an inhouse sample prepared according to previously described methods.^{11, 12}

Dextran T-2000 ($M_w = 2\,000\,000$ g/mol) was purchased from Pharmacia Fine Chemicals. Maltotriose, trigalacturonic acid, adipic acid dihydrazide (ADH), O,O'-1,3,-propanediylbishydroxylamine dihydrochloride (PDHA) and 2-methylpyridine borane complex (α -picoline borane) was purchased from Sigma-Aldrich. PEG linkers were purchased from BroadPharma, US. All other chemicals were obtained from commercial sources and of analytical grade.

Semi-preparative gel filtration chromatograph (GFC)

Three Superdex 30 (preparative grade) columns (HiLoad 26/60, 26 mm x 60 cm, GE Healthcare Life sciences) were connected in series. The mobile phase (0.1 M ammonium acetate (AmAc), pH 6.9) was eluted at a flow rate of 0.8 ml/min. Samples (0.3 – 65 mg/ml) were dissolved in the mobile phase and injected. The separation was monitored by an on-line RI detector (Shodex R1-101). Fractions were collected (4 – 8 ml per fraction) and pooled according to elution volume. Fractions were dialysed ($DP_n < 7$ with 100 – 500 Da MWCO and $DP_n \geq 7$ with 3.5 kDa MWCO) against 50 mM NaCl (2 shifts) and MQ until the conductivity was below 2 μ S and freeze-dried.

NMR spectroscopy

Alginate samples were dissolved in 470 – 500 μ l D_2O (99.9% D; Sigma-Aldrich) (10 – 12 mg/ml). For samples where pD was adjusted, DCl or NaOD was used. Samples were either analysed at the temperature 25 °C, 27 °C, or 82 °C.

Homo- and heteronuclear NMR were recorded on a Ascend 400 MHz Avance III HD instrument equipped with a 5 mm SmartProbe, Advance ultra-shield 600 MHz Avance III HD instrument equipped with 5 mm cryogenic CP-TCI, Bruker Ascend 600 MHz NEO instrument equipped with 5 mm iProbe or a Ascend 800 MHz Avance III HD instrument equipped with 5 mm cryogenic CP-TCI all from Bruker BioSpin AG, Fällanden, Switzerland.

Characterization of alginate oligomers was performed by obtaining 1D ^1H -NMR spectra at 25 °C or 82 °C on the 400 MHz or NEO 600 MHz, or at 27 °C on the 600 MHz with cryogenic probe.

Time course NMR experiments was performed by obtaining 1D ^1H -NMR spectra at set time points over the course of the reaction on the 600 MHz with cryogenic probe at 27 °C or the NEO 600 MHz at 25 °C. Spectra were recorded every 30-40 min for the first 3 hours, then every 1 – 3 hours until equilibrium was established. Reactions were performed in deuterated acetate buffer (500 mM, pD 4 and 5). TSP was added to a final concentration of 2 mM. The pD was adjusted with 1 M NaOD and the measured pH* (by the instrument calibrated by non-deuterated standards) was corrected as follows; $\text{pH} = 0.9291 \times \text{pH}^* + 0.421$.¹³ Guluronate oligomers (G_n), mannuronate oligomers (M_n), dextran oligomers (Dex_m), maltotriose (Glc_3) and galacturonic acid (GalA_3) (7 – 20.1 mM) and 2 or 10 equivalents ADH or PDHA was dissolved in NaAc-buffer. Reduction of conjugates was studied by adding PB (3 equivalents) to the NMR tube. Integration was used to estimate the relative molar ratios of reactants and products (using either ^1H of the non-reducing end or TSP as internal standard).

Chemical shift assignment of equilibrium reaction mixtures was recorded on the NEO 600 MHz at 25 °C or 82 °C by acquiring the following spectra: 1D ^1H , 2D ^{13}C Heteronuclear Single Quantum Coherence (HSQC) with multiplicity editing, 2D Double Quantum Filtered Correlation Spectroscopy (DQF-COSY), 2D ^{13}C Heteronuclear 2 Bond Correlation (H2BC) and 2D ^{13}C heteronuclear multiple bond correlation (HMBC).

1D selective pulse program with gradient selection COSY (pulse program: selcogp) and Total Correlation Spectroscopy TOCSY (pulse program: seldigpzs) was acquired on the 800 MHz at 25 °C.

Chemical shift assignment of purified conjugates was done using the 800 MHz at 25 °C by acquiring the following spectra: 1D ^1H , DQF-COSY, HSQC with multiplicity editing, 2D ^{13}C HSQC- $[\text{}^1\text{H}, \text{}^1\text{H}]$ TOCSY, 2D H2BC and 2D HMBC.

All data were recorded, processed and analysed using TopSpin software version 3.5pl7 or 3.6.1 (Bruker BioSpin).

SEC-MALS

Molar masses and intrinsic viscosities were analysed by Size Exclusion Chromatography (SEC) with Multiangle Light Scattering (MALS). Samples were dissolved in the mobile phase (0.15 M NaNO_3 with 10 mM EDTA) and filtered (0.45 μm) prior to injection. An Agilent Technologies 1260 IsoPump with a 1260 HiP degasser was used to maintain a flow of 0.5 ml/min during analyses. 50 – 100 μl were injected from an Agilent Technologies Vialsampler. TKS Gel columns 4000 and 2500 PWXL were connected in series. DAWN Heleos-II and ViscoStar II detectors from Wyatt Technology were connected in series with a Shodex refractive index detector (RI-5011). Astra 7.3.0 software was used for data collection and processing.

Preparation of oligouronate conjugates

For preparative purposes, guluronate (G) or mannuronate (M) oligomers (20.1 mM) were dissolved in NaAc-buffer (500 mM, pH 4) and 10 equivalents PDHA/ADH (201.0 mM) were added. After about 24 h, 3 equivalents (60.3 mM) of α -picoline borane (PB) were added. The mixture was left at room temperature for 120, 22, 39 and 12 hours for G_n -PDHA, M_n -PDHA, G_n -ADH and M_n -ADH, respectively. Samples were placed on shaking during reduction. The reaction was terminated by dialysis (for $\text{DP}_n < 7$ with 100 – 500

Da MWCO and for $DP_n \geq 7$ with 3.5 kDa MWCO) against 50 mM NaCl until all insoluble PB had been removed. The solution was subsequently dialysed against MQ water for 2 – 5 h to remove high excess salt before the solution was freeze dried. The conjugates were subsequently purified by GFC.

Reduction of conjugates at elevated temperatures

Oligoguluronate (20.1 mM) was dissolved in deuterated NaAc-buffer (500 mM, pD 4.0) and PDHA (40.2 mM) was added. After 24 h, 60.3 mM (3 equiv.) PB was added, and the reaction mixture was placed in a water bath (preheated to 40 °C). After 6, 10, 21 and 24 hours, samples (0.5 ml) were taken and analysed by ^1H 1D NMR, the yield (%) of reduced conjugates was obtained by integration.

Preparation of oligoguluronate diblocks ($G_n\text{-b-G}_n$)

A guluronate decamer (G_{10}) (DP determined by ^1H 1D NMR) was dissolved in NaAc-buffer (500 mM, pH 4.0) to a concentration of 20.1 mM. 0.5 equivalents ADH was added to the solution and the reaction was placed on shaking for 24 h at room temperature. Six equivalents of (solid) PB (120.6 mM) were added. The mixture was further shaken for up to 40 hours. The reduction was terminated by dialysis against 50 mM NaCl (3.5 kDa MWCO), removing any solid PB from the reaction mixture. The solution was subsequently dialysed against MQ water for 2 – 5 h and freeze dried. The diblocks were purified by GFC.

Preparation of guluronate-b-dextran ($G_n\text{-b-Dex}_m$) block copolymers

$G_n\text{-b-Dex}_m$ were prepared in two steps. High molecular weight dextran (T-2000) was partially hydrolysed in 0.05 M HCl at 95 °C to obtain DP_n (by NMR¹⁴⁻¹⁶) of ca. 34 (2.25 h) and 18 (6 h). Following cooling and neutralization (with dilute NaOH), the solution was dialysed (3.5 kDa MWCO) and freeze dried. They were further activated with PDHA prior to fractionation as described previously.⁷ In brief, dextran was dissolved in NaAc-buffer (500 mM, pH 4.0) to a concentration of 10 mM and 10 equivalents

of PDHA (100 mM) were added. After 24 h, 20 equivalents of PB (200 mM) were added and the reaction proceeded at 40 °C for 24 hours. The reaction was terminated by dialysis and freeze drying. Narrow molar mass fractions were further prepared by semi preparative GFC as described above. Fractions were freeze dried directly, removing volatile AmAc, and characterized by ^1H 1D NMR and SEC-MALS. In the second step, defined fractions of dextran-PDHA (7 mM) were dissolved in NaAc buffer (500 mM, pH 4.0) and oligoguluronate (21 mM) was added. The solution was shaken overnight before 3 equivalents of PB (63 mM) were added. The reaction was left on shaking for 120 hours before it was terminated by dialysis (3.5 kDa MWCO) against 50 mM NaCl and freeze dried. The block copolymer was purified by GFC.

Solubility and particle formation of oligoguluronate-b-dextran monitored by DLS

G_n - b -Dex $_m$ diblocks ($n = 10, 40$ and $m = 100$) (10 mg/ml) were dissolved in 1 ml 10 mM NaCl overnight before filtering (0.22 μm). After 24 h, the sample was dialysed (Float-A-Lyser 100 – 500 Da) against 20 mM CaCl_2 containing 10 mM NaCl (1 L). Samples (50 - 100 μL) were taken regular time intervals. The scattering intensity (kilo counts per second, kcps) and intensity distribution were determined using a ZetaSizer Nano ZS (Malvern Instruments, UK) (25 °C, $\lambda = 632.8$) with back scattering detection (173°). The number distribution was calculated assuming that the refractive index (1.590) and absorption factor (0.010) of polystyrene latex could be used. All samples were analysed using 8 runs with duration of 30 – 40 sec. All samples were analysed by minimum 5 consecutive measurements. Data were acquired and analysed using Malvern Zetasizer Software Version 7.12.

Results and discussion

The chemistry and reaction kinetics of the reaction at the reducing ends of oligoguluronate and oligomannuronate with a dioxyamine (PDHA) and a dihydrazide (ADH) were first studied using trimers (G_3 and M_3) as model systems. Short oligomers ease the NMR characterisation, and the findings can

further be compared to previously reported data for dextran, chitosan and chitins.^{7, 8} The reaction schemes for conjugation with guluronate and PDHA/ADH, including the reduction of Schiff bases to the stable secondary amines, are shown in Fig. 2.

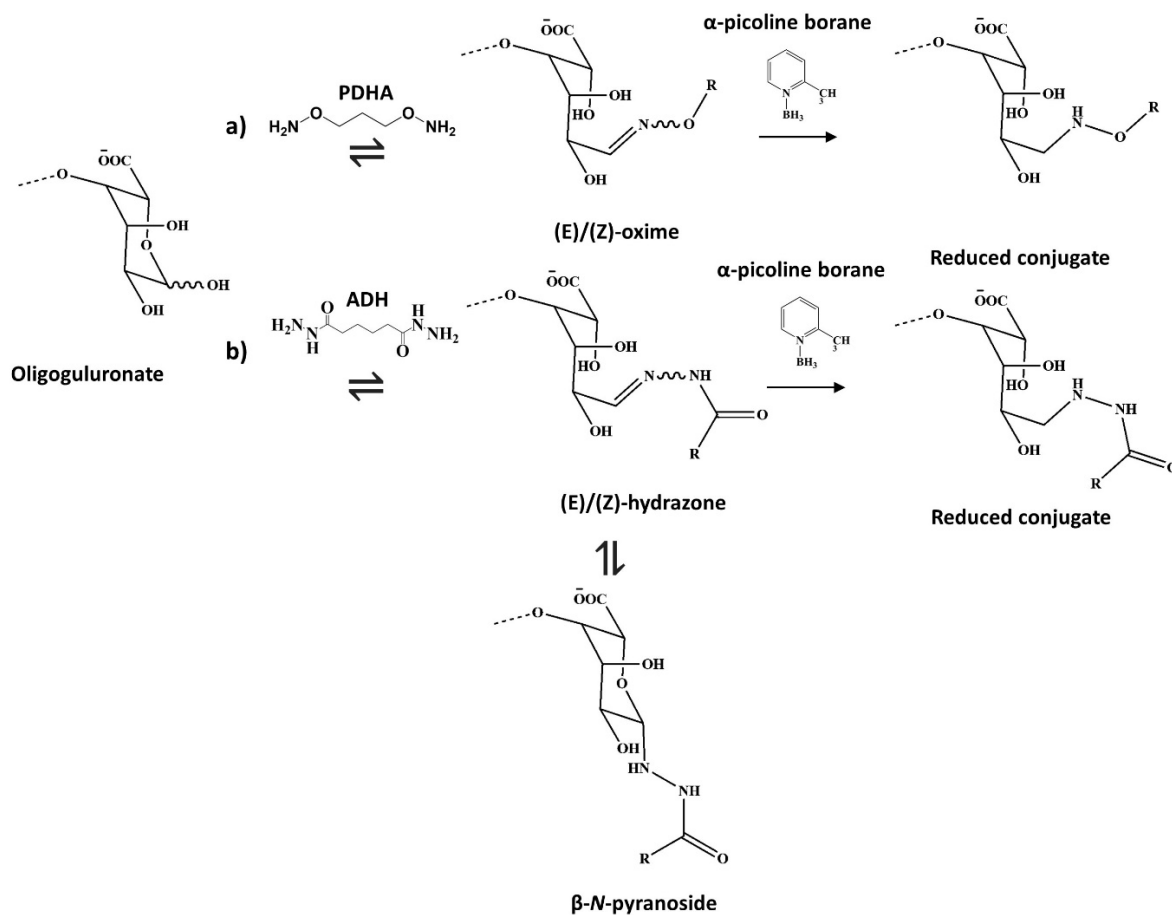


Fig. 2 Schematic overview of the reducing modifications of oligoguluronate (G_n) with a) O,O'-1,3,-propanediylbishydroxylamine dihydrochloride (PDHA), and b) adipic acid dihydrazide (ADH), and the reduction of the Schiff bases to stable, secondary amines using α-picoline borane as reductant.

Pure oligomannuronate and oligoguluronate blocks were prepared by conventional methods based on partial hydrolysis and pH-dependent fractional precipitation (Fig. S2[†]).^{12, 17-19} Initial conditions for conjugation were otherwise identical to previous studies of dextran and chitin/chitosan oligomers,^{7, 8} i.e. 500 mM acetate (strong buffering needed, especially for oxyamines¹³) pH 4.0, room temperature (RT).^{7, 8, 13} The reactions were systematically monitored by recording NMR spectra at regular intervals until equilibrium was established. However, with previously used standard conditions (20 mM oligomer and 10 equivalents of PDHA/ADH) the reactions turned out to be too fast for accurate determination of the kinetics of reaction by time course NMR. Subsequent studies were mostly conducted at 7 mM oligomer with 2 equivalents PDHA/ADH.

Conjugation with PDHA

Results for the G₃-PDHA system at equilibrium (with 2 equivalents PDHA) are shown in Fig. 3a. The ¹H-NMR spectrum includes annotations of the major resonances. Complete disappearance of reducing end signals is balanced by the appearance of E- and Z-oximes (2:1 molar ratio) (Fig. S4 - S7[†]). N-pyranosides could hence not be found, which seems to be rare for hexoses, and to our knowledge only reported for a mannose-oxyamine system.¹³ The reaction was indeed rapid as equilibrium was established already after 90 minutes. The equilibrium reaction mixture was further analysed by 2D NMR (Fig. S5a[†]) to resolve and assign resonances that were partially overlapping in 1D NMR. Minor forms of E and Z oximes (approximately 5%) appeared at slightly higher chemical shifts than the main peaks (annotated (E')/(Z')-oximes in Fig. 3a). When purifying unreduced G₃-PDHA by GFC and dialysis, the relative amount of the minor forms increased considerably. Their presence was, however, independent of pH in the range 6 – 11.8 (Fig. S5b[†]), precluding lactonization as a possible explanation. The detailed chemistry of the minor

forms is hence not understood at this time, however, both forms do become reduced in the presence of PB (see below).

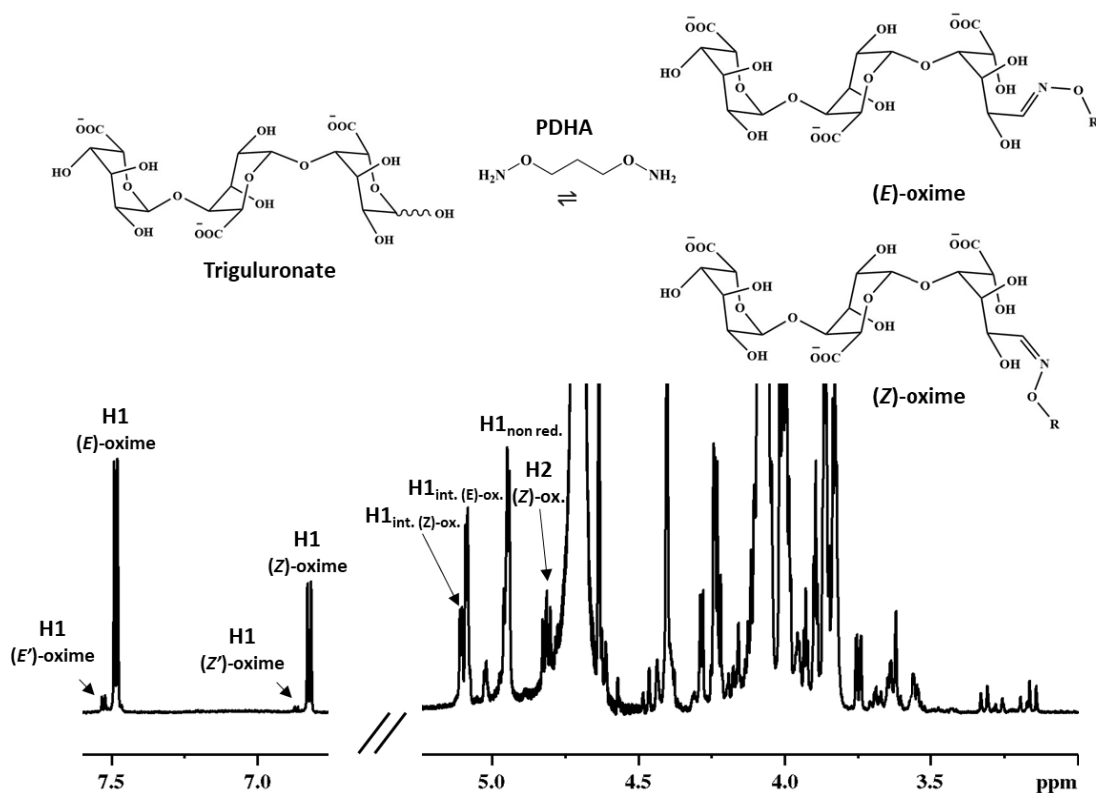
A kinetic plot for the conjugation with G₃ and PDHA (2 equiv.) is shown in the Supplementary Information (Fig. S6[†]). The experimental data were fitted to a simplified kinetic model described in detail previously,⁸ providing rate constants (k_T and k_{-T}) for the combined yield (total oximes) of the reaction, i.e. by treating the reaction products as a single component.⁷ The reaction rates were taken to be first order with respect to the concentrations of the reactants.⁷ Indeed, as shown in the Supplementary Information (Fig. S6-S17[†]), all experiments were well described by the model. It can in particular be used to predict the kinetics when concentrations have to be changed, for example for longer DPs. By the same model, the times for reaching 50% and 90% of the equilibrium yield ($t_{0.5}$ and $t_{0.9}$) were obtained. They turned out to be 10-15 times shorter than for a dextran trisaccharide conjugated to PDHA under identical concentrations and conditions (Fig. S9[†]). Hence, the fast reaction and excellent yield both qualify for the term 'oxime click' in this case. Being in addition aniline free and copper-free the 'oxime click' method is well suited for oligoguluronate.

To investigate the role of DP the reaction was studied with an oligoguluronate with DP 8. Under otherwise equal conditions the octamer reacted about two times slower than the trimer (Fig. S8[†]). Higher DPs were investigated but gave progressively less quantifiable peak integrals in NMR (broad peaks being too close to the HDO resonance). However, complete PDHA-conjugated oligoguluronate with higher DP could indeed be prepared as shown below.

The reaction was also studied at pD 5 (otherwise identical conditions). Complete conversion was obtained also here (Fig. S10[†]), but the rate of the reaction was about 3 times lower than at pD 4 (Fig. S11[†]). Lowering pH is known to increase the reaction rate but reduce the yield.^{8, 13} Hence, pD 4 is preferred as it provides sufficiently rapid reaction without entering the range where longer oligoguluronates become protonated and insoluble.²⁰

Corresponding results for trimannuronate (M_3) with PDHA are shown in Fig. 3b. Oxime resonance structures analogous to those of G_3 -PDHA were observed. The E/Z ratio was 4:1, which is twice what has been observed for oligoguluronate. Also in this case, (E) and (Z)-oximes were almost exclusively formed, with minor forms (E'/Z') accounting for about 5%. A combination of 1D selective COSY, TOCSY, and 2D heteronuclear NMR spectra was used to verify the structure of purified M_3 -PDHA (Fig. S13-14[†]). The kinetics was otherwise quite similar what was obtained for G_3 (Table 1) (Fig. S15[†]).

a)



b)

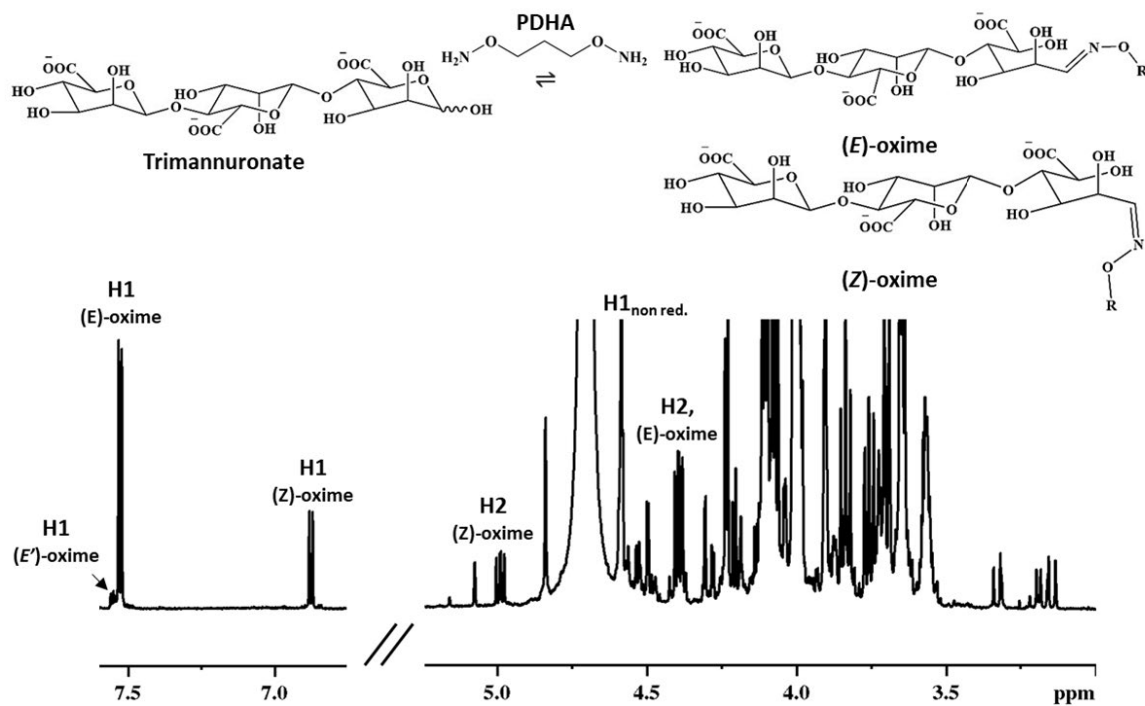


Fig. 3 Reaction schemes and ^1H -NMR spectra of the equilibrium reaction mixture for the reaction with a) oligoguluronate G_3 and b) oligomannuronate M_3 with PDHA (2 equiv.) in 500 mM AcOHd_4 , pD 4 recorded at 800 MHz and 25 °C and 600 MHz and 27 °C, respectively. Chemical shifts of key resonances are annotated as follows: non. red. indicates the non-reducing end. Int. indicates the residue closest to the reducing end. Complete assignment of chemical shift for the modified reducing end is provided in Supplementary Information (Fig. S5a - b[†] and Fig. S14[†]).

Table 1. Reactions with alginate oligomers with 2 equivalents PDHA studied by time course NMR.

Rate constant (k_T) is based on a first order kinetics model for combined yield (%). The reactions were studied at room temperature. Dextran (Dex_m) and maltotriose (Glc_m) is included as a comparison. (n.d.: Could not be accurately determined because of yields close to 100%). Values marked with an asterisk (*) are recalculated from k_T and k_{-T} values obtained at 20.1 mM.

Oligomer	Oligomer conc. [mM]	pD	AcOH[d ₄] [mM]	Ratio <i>E:Z:β-N-pyr.</i>	$t_{0.5}$ [h]	$t_{0.9}$ [h]	k_T	k_{-T}	Equil. conversion (%)
G_3	7.0	4	500	2.2:1:0	0.29	1.06	8.7×10^{-2}	7.7×10^{-2}	92
M_3	7.0	4	500	2.6:1:0	0.17	0.62	1.6×10^{-1}	n.d.	94
G_8	7.0	4	500	2.1:1:0	0.40	1.45	6.4×10^{-2}	4.1×10^{-2}	97
G_3	7.0	5	500	2.6:1:0	0.75	2.67	3.1×10^{-2}	8.7×10^{-2}	93
G_6	20.1	4	500	2.2:1:0	0.38	1.39	2.4×10^{-2}	n.d.	92
	7.0*				1.10*	4.01*			
Dex_3	7.0	4	500	4.1:1:1	4.55	14.76	4.4×10^{-3}	2.4×10^{-2}	77
Glc_3	7.0	4	500	3.1:1:1.6	4.02	13.26	4.0×10^{-3}	5.1×10^{-2}	63

Conjugation with ADH

Conjugation with oligoguluronate and oligomannuronate with ADH was studied using a similar approach as described for PDHA. For oligoguluronates only small amounts (< 5%) corresponding to (E) or (Z) hydrazones were observed, whereas a major resonance appeared in ^1H -NMR as a doublet at 4.28 ppm ($^3J_{(\text{H1-H2})}$ 9.54 Hz (Fig. 4a), in agreement with the formation of β -*N*-pyranosides. This is in line with conjugation of hydrazides and other reducing sugars, for example ADH-conjugated dextran.^{7, 8, 21} The reaction reached equilibrium after 1.5 h (Fig. S16[†]). However, the total conversion was only 48% with 7 mM oligoguluronate and 2 equiv. of ADH. This is also in agreement with previous findings for ADH conjugation to oligosaccharides.⁸ The rate constants are included in Table 2, and the kinetic plot is included in Supplementary Information (Fig. S17[†]). To obtain higher conversion an experiment with G_6 (20.1 mM) using 10 equiv. of ADH was conducted. A yield 88% was obtained after 8 h, which fits well with the predicted yield (87%) estimated by the kinetic model.

The conjugation of ADH to oligomannuronates turned out to be somewhat different from that of oligoguluronates. Contrary to oligoguluronates, significant amounts of hydrazones were in this case detected by characteristic resonances⁷ at 7.3 and 7.6 ppm (Fig. 4 and Fig. S18[†]). *N*-pyranosides normally have resonances in the 3.8 – 4.5 ppm region,^{7, 21} but due to peak overlap these resonances could not be directly identified in this case. However, their presence was estimated to account for about 20% based on difference in the decrease of the reducing end and the increase of the hydrazone signals. When increasing to 10 equivalents ADH the combined yield reached 92% (Fig. S19[†]), which is higher than predicted by the model (81%). However, integration of signals was difficult and may have affected the estimated yield. Results are included in Table 2.

Attempts were made to purify the M_n-ADH conjugates by GFC (pH 6.9) followed by dialysis and freeze drying. However, this led unexpectedly to complete loss of linked ADH and recovery only of unconjugated oligomannuronate, most probably due to reversal when the excess ADH is removed in the dialysis. However, as will be shown below, stable M_n-ADH conjugates can be obtained in high yields when combined with a reduction step. In contrast, unreduced G_n-ADH conjugates seemed to be stable in this process.

The differences between oligoguluronates and oligomannuronates in terms of ADH conjugation raises the question how other uronates may react. To test this a conjugation reaction was performed with a trigalacturonate (GalA₃). Results are included in Table 2 and in Supplementary Information (Fig. S20[†]). Trigalacturonate behaved quite similarly to the two others. The relative amount of the cyclic β-N-pyranoside was higher than for oligomannuronate, but lower than for oligoguluronate. Taken together, these findings are unforeseen and indicate that the reaction with ADH, in contrast to PDHA, must depend on the detailed chemistry at some distance from the carbonyl group involved in the reactions provided the reacting sugars exist in the open chain form (Fig. 2). Specifically, the open chain forms of the reducing ends of M and G residues are identical at C1-C4, and at C5 only the stereochemistry is different.

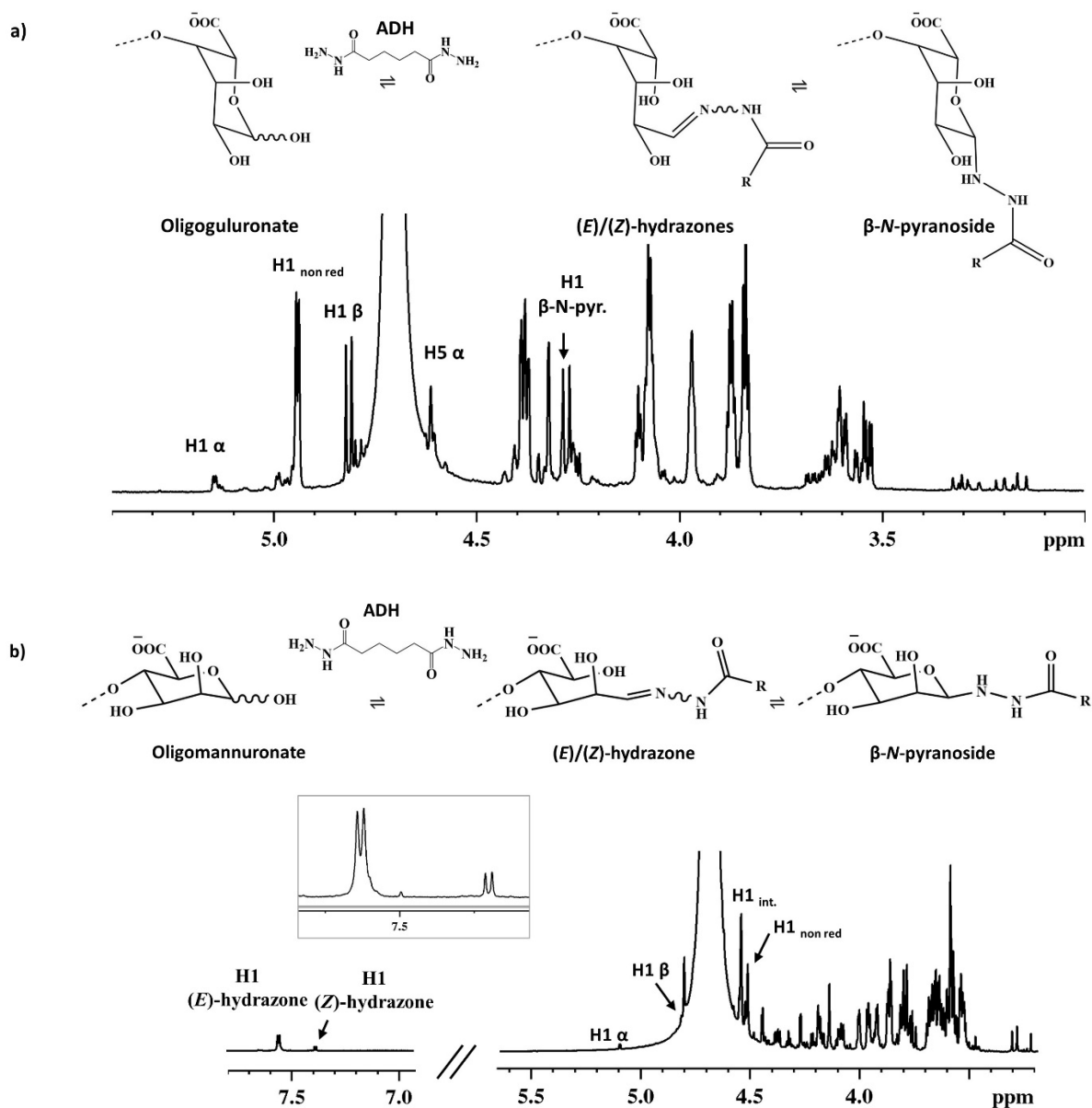


Fig. 4 Reaction schemes and ^1H -NMR spectra of the equilibrium reaction mixture for the reaction of a) oligoguluronate (spectrum for G_2 shown) and b) oligomannuronate (spectrum for M_3 shown) with ADH (2 equiv. and 10 equiv., respectively) in 500 mM AcOHd_4 , pD 4 recorded at 600 MHz and 27 °C. Key resonances are annotated as follows: non. red. indicates the non-reducing end. Int. indicates the residue closest to the reducing end.

Table 2. Reactions of alginate oligomers with ADH studied by time course NMR. The rate constants (k_T and k_{-T}) are based on the first order kinetics model for the combined yield. Values marked with an asterisk (*) are recalculated from k_T and k_{-T} values obtained for 20.1 mM of oligomer and 2 equivalents of ADH. n.d.: the reaction was too fast to accurately monitor by NMR.

Oligomer	ADH equiv.	Oligomer conc. [mM]	pD	AcOH[d ₄] [mM]	Ratio E:Z:β-N-pyr.	t _{0.5} [h]	t _{0.9} [h]	k _T	k _{-T}	Eq. yield (%)
G ₂	2	7.0	4.0	500	1:0.2:32	0.39	1.33	3.0x10 ⁻²	8.2x10 ⁻¹	48
G ₆	10	20.1	4.0	500	1:0.1:26	0.10	0.34	3.1x10 ⁻²	7.7x10 ⁻¹	88
	2*	7.0*				0.40*	1.36*			
M ₃	2	7.0	4.0	500	1:0.3:1.6	0.55	1.85	1.6x10 ⁻²	7.4x10 ⁻¹	36**
M ₃	10	20.1	4.0	500	1:0.1:1.1	n.d.	n.d.	n.d.	n.d.	92**
GalA ₃	2	7.0	4.0	500	1:0.2:8	0.23	0.84	4.95x10 ⁻²	7.76x10 ⁻¹	64

The data show that although having different reaction kinetics and distribution of conjugates (E- and Z-conjugates, and N-pyranosides) both ADH and PDHA can fully conjugate to oligouronates when proper conditions are met. It should be noted that for preparative purposes, 10 equivalents of PDHA/ADH is preferred in order to minimise the formation of doubly substituted conjugates.⁷ However, even when using 10 equivalents, 5 – 10% doubly substituted conjugates are formed. These can, however, be easily removed during purification (Fig. S21†).

Attachment of the second block: A-*b*-B diblock polysaccharides:

The high reactivity of oligouronates with PDHA implies that reaction with PDHA-activated oligosaccharides to obtain diblock oligo- or polysaccharides would proceed equally well. This was tested in kinetic studies with dextran-PDHA (DP 10), maltotriose-PDHA (DP 3), β -1,3-glucan-PDHA (DP 9) and chitin-PDHA (A_nM type)⁷ (DP 5). Here, A stands for N-acetyl-D-glucosamine and M signifies the reactive terminal 2,5-anhydro-D-mannose (generally denoted M in the literature) at the reducing end. In addition, the reaction was also studied with G_n -PDHA for preparation of symmetrical blocks. All conjugates had been fully reduced with PB prior to coupling with oligogulonate.^{7,8} These PDHA-activated oligosaccharides represent widely different chemistries (Table 3): Dextrans are neutral chains with high chain flexibility due to α -1,6 linkages. Chitins are uncharged but more rigid and hydrophobic and can self-assemble (crystallise) at higher DPs. Amylose (α -1,4-linked glucans) and β -1,3-glucans are both semi-rigid, neutral chains with the ability to form higher order structures. Collectively they illustrate the versatility of the approach towards almost any type of diblock polysaccharides.

The conjugations with oligogulonates were initially studied using a 1:1 or 2:1 molar ratio between the reactants. Fig. 5 shows NMR spectra of Dex₁₀-PDHA (PDHA conjugated dextran decamer) before and after further conjugation to G_3 . Results for all PDHA-activated oligosaccharides are summarized in Table 4. Several PDHA-oligosaccharides react with G_n with rates similar to those of free PDHA, except for PDHA-activated chitin oligomer, which is a factor two slower (Table 1). Another exception was PDHA-maltotriose, which for presently unknown reasons did not seem to react (Fig. S22[†]). Yields were otherwise in the range 40 - 60%. The preparation of diblock polysaccharides with reduction and purification is further described in detail below.

Table 3. Coupling of PDHA-activated oligosaccharides to oligogulonates (G₃).

Activated block (A*)	Second block (B)	Ratio (A*-B)	Conc. of B [mM]	Equ. yield (%)	k _T	k _{-T}	t _{0.5} [h]	t _{0.9} [h]
G ₁₀ -PDHA	G ₃	1:1	7.0	45	3.3x10 ⁻²	1.6x10 ⁻¹	1.4	5.1
Dex ₁₀ -PDHA	G ₃	1:1	7.0	42	7.1x10 ⁻²	3.8x10 ⁻¹	0.6	2.2
A ₄ M-PDHA	G ₂	1:1	20.1	57	8.0x10 ⁻³	5.1x10 ⁻²	2.7	10.1
b-1,3-glucan-PDHA	G ₃	1:1	7.0	61	8.0x10 ⁻²	1.4x10 ⁻¹	0.9	3.3
G ₇	aminoxy-PEG-N ₃	1:2	20.1	94	4.4x10 ⁻²	3.3x10 ⁻³	0.16	1.79

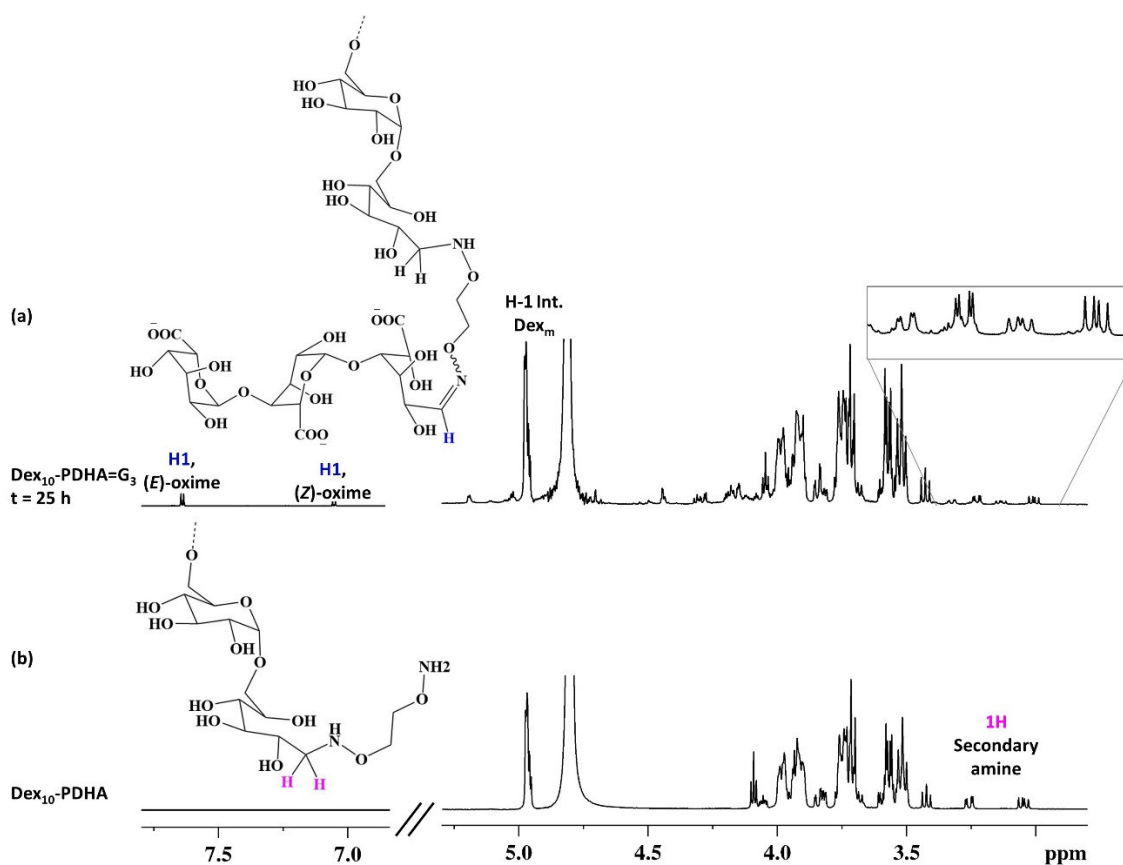


Fig. 5 ¹H-NMR spectra of the equilibrium reaction mixture with G₃ and PDHA-Dex₁₀ (1:1) in 500 mM AcOH[d₄] pD 4 (NEO 600 MHz) at 25 °C. Resonances from (E)/(Z)-oximes of the conjugate are

annotated. The structure of the conjugated $G_n=b\text{-Dex}_m$ is included (= refers to unreduced oxime). ^1H -NMR spectra of purified $\text{Dex}_{10}\text{-PDHA}$ is included for comparison.

Reduction of oximes/hydrazones/N-pyranosides with α -picoline borane

Although the non-reduced oximes/hydrazones/N-pyranosides may sometime be useful, for instance by taking advantage of their reversibility,⁵ many applications will require reduction for better stability. Reduction also reduces the structural complexity when secondary amines are formed. Although only oximes and hydrazones are reduced directly, the principle of Le Châtelier ensures that the N-pyranosides revert to the parent oximes/hydrazones and are therefore reduced (Fig. 2).

Reduction kinetics was initially studied by adding 3 equivalents of PB to the equilibrium reaction mixtures of four chosen oxime/hydrazone model systems ($G_2\text{-PDHA}$, $G_3\text{-ADH}$, $M_3\text{-PDHA}$ and $M_3\text{-ADH}$). Reduction was observed by the gradual disappearance of oxime/hydrazone/N-pyranoside resonances during time course NMR, and the corresponding emergence of methylene protons.⁸ For all systems, complete conversion to the secondary amine was obtained (Fig. S25-S28[†]). Reduction data are given in Table 4.

For $M_3\text{-PDHA}$ the reduction was complete after ca. 22 hours, whereas $G_2\text{-PDHA}$ needed ca. 120 hours under the same conditions. Both samples were purified by GFC for further structural characterization. For $G_2\text{-PDHA}$, multiple forms were present at pH 5, as evident by multiple signals from the methylene protons in the range 2.8 – 3.5 ppm. However, by adjusting to pH 10, only a single resonance from each methylene proton was observed (Fig. S32[†]). 1D selective COSY and TOCSY NMR was used for chemical shift assignment of key resonances at pH 5 and 10 (Fig. S29-S30[†] and Tables S3-S4[†]). For $M_3\text{-PDHA}$, the

same trend was observed (Fig. S31[†] and Table S5[†]). The multiple forms observed at pH 5 could possibly be the result of lactonization involving the reducing ends.²²

For G₃-PDHA, reduction was also investigated at 40 °C in order to possibly increase the reaction rate. In this case PB was added in two portions (after 0 and 10 h), because the rate of decomposition of PB increases with temperature.⁸ After 24 h complete conversion to secondary amine was obtained. Such reduction times are considered acceptable for most protocols, and the alginate-based oximes are in any case reduced much faster than e.g. chitin/chitosan-based oximes,⁸ as well as dextran-PDHA conjugates.⁷ It should be noted that at 40 °C some reduction of the reducing end aldehyde of oligoguluronates themselves indeed takes place. This demonstrated using 20 equivalents of PB, which resulted in approximately 50 - 60% reduction of the reducing end aldehyde after 24 h (Fig. S33[†]). Therefore, when using elevated temperatures for the reduction, a general two-step protocol using first 10 equivalents of PDHA to obtain complete conversion to oximes (at room temperature) prior to the reduction step, is recommended.

Reduction of M_n-ADH was more rapid than for G_n-ADH. The former was fully reduced after 12 h and the latter after 39 h. This is reasonable since M_n-ADH has a higher proportion of directly reducible hydrazones. Both systems are reduced much faster than Dex_m-ADH and chitosan-ADH (D_nXA type).⁸

Table 4. Reaction conditions for the reduction of equilibrium reaction mixtures of M_n-PDHA, G_n-PDHA, G_n-ADH and M_n-ADH with 3 equiv. PB to obtain complete conversion (%). The reduction was studied

by monitoring the change in (E)/(Z)-oximes/hydrazones and N-pyranoside by ^1H -NMR. The ^1H -NMR spectra are included in Supplementary Information (Fig. S25-S28†).

Reaction	T [°C]	Reduction time [h]
G ₂ -PDHA	22	120
M ₃ -PDHA	22	22
G ₃ -PDHA	40	24
G ₂ -ADH	22	39
M ₃ -ADH	22	12

The reduction was also studied for a system of G₇ and aminoxy-PEG₅-N₃ (Fig. S34†). The reduction followed the trend observed with PDHA, and fully reduced conjugates could be prepared. This shows the general applicability of reductive amination of alginates with oximes and also opens for (Cu-free) azide-alkyne chemistry at the reducing end.

Alginate-based diblock polysaccharides

The results above show that fully reduced oligoguluronate based conjugates can be readily prepared. We applied this approach to prepare different diblocks with oligoguluronate. We first prepared the symmetric G₁₀-ADH-G₁₀ diblock by employing 0.5 equivalents of ADH followed by reduction with PB. The diblock was purified by GFC (Fig. 6a) and the structure was verified by NMR (Fig. 6b). Integration show polymerization of ADH, a reaction that has previously been reported.⁸ The yield of the diblock was estimated to 50 – 60% based on SEC chromatogram. The samples were subsequently studied by multidetector SEC (Fig. 6c) providing molar mass distributions as well as intrinsic viscosity distributions

(Table 5), whereas radii of gyration cannot be obtained in this case because of the limited size compared to the wavelength of the laser. A symmetrical diblock was prepared with G₁₀ and PDHA using the same approach. The SEC-MALS analysis provided intrinsic viscosity in agreement with a broken rod architecture in line with the findings for the G₁₀-ADH-G₁₀ block (Fig. S35[†] and Table S6[†]).

Table 5. Molar mass averages of a G₁₀-*b*-G₁₀ block (after purification by GFC) and the starting material (G₁₀). G₂₃ is included for comparison of intrinsic viscosities (see text). The data were obtained from SEC-MALS with an in-line viscosity detector.

Sample	M _n (kDa)	M _w (kDa)	DP _n	[η] _w (mL/g)
G ₁₀	2.0	2.1	10	7
G ₁₀ -ADH-G ₁₀	3.8	3.9	19	10
G ₂₃	4.5	4.6	23	15

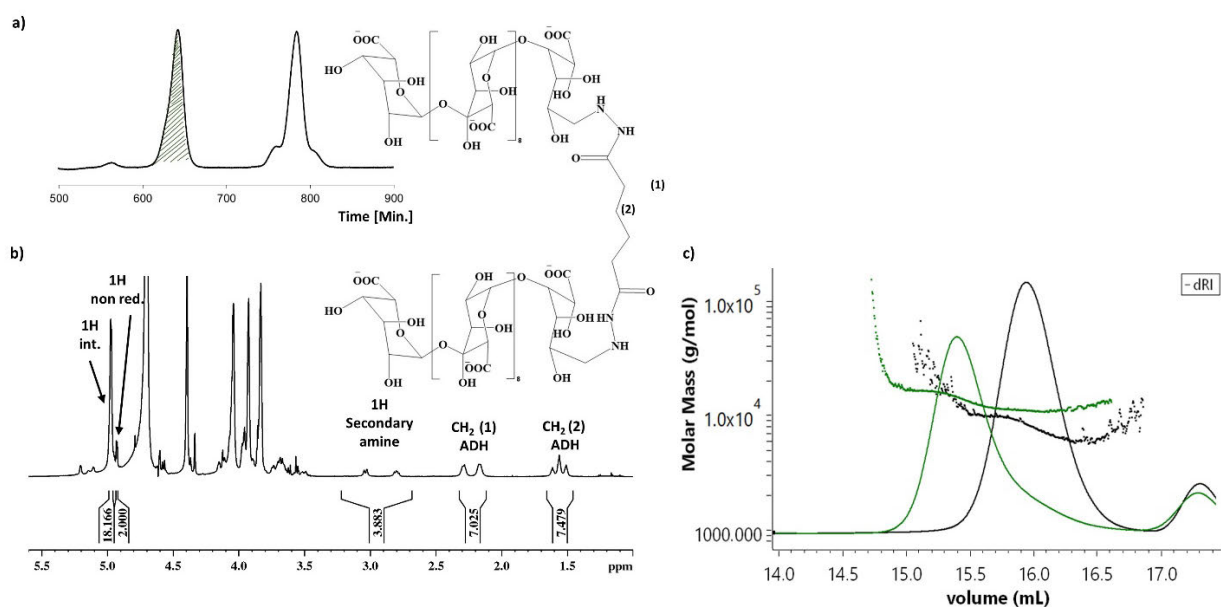


Fig. 6 A symmetrical G₁₀-ADH-G₁₀ diblock was prepared and purified by GFC (a, hatched area) and analysed by ¹H NMR (600 MHz, 25 °C) (b) and SEC-MALS (c). The latter included G₁₀ (black) and G₂₃ (not shown). The coupling was manifested by a marked shift in elution volume and doubling of the molar mass. Intrinsic viscosity data were simultaneously obtained by an in-line viscosity detector, and revealed the effect of the high flexibility of the linker region compared to the G-blocks (see text). All values are summarized in Table 5.

Data show the expected doubling of molar mass and retention of the narrow molar mass distribution of the starting materials. Interestingly, the intrinsic viscosity of the diblock was only about 1.5 times higher than that of G₁₀, and only 2/3 of that of G₂₃. Alginates have under the SEC-MALS conditions a persistence length of about 15 nm.²³ With an estimated length of each G residue of 4.35 nm,²⁴ G₁₀ becomes relatively rod-like, whereas the flexible spacer (ADH) and the two terminal guluronates (in the open chain form) have single bonds with large conformational freedom. The diblock therefore approaches a broken rod type geometry. Future studies will therefore try to clarify the role of such architectures in gel formation, Ca²⁺ binding etc. in comparison to the known roles of pure oligoguluronates as calcium alginate gel modifiers.^{25, 26}

To demonstrate the applicability of the conjugation protocols to long chains the G₁₂-PDHA-Dex₁₀₀ diblock was prepared by reacting free G₁₂ with purified PDHA-dextran with DP_n of 100. Three equivalents of G₁₂ were here chosen to ensure quantitative substitution of the PDHA-dextran. Residual (unreacted) G₁₂ was selectively removed by GFC (Fig. 7a). SEC-MALS data for the diblock showed a clear shift in elution profile compared to the free blocks (Fig. 7b). The molar masses obtained by SEC-MALS (Table 6) agreed well with the theoretical values.

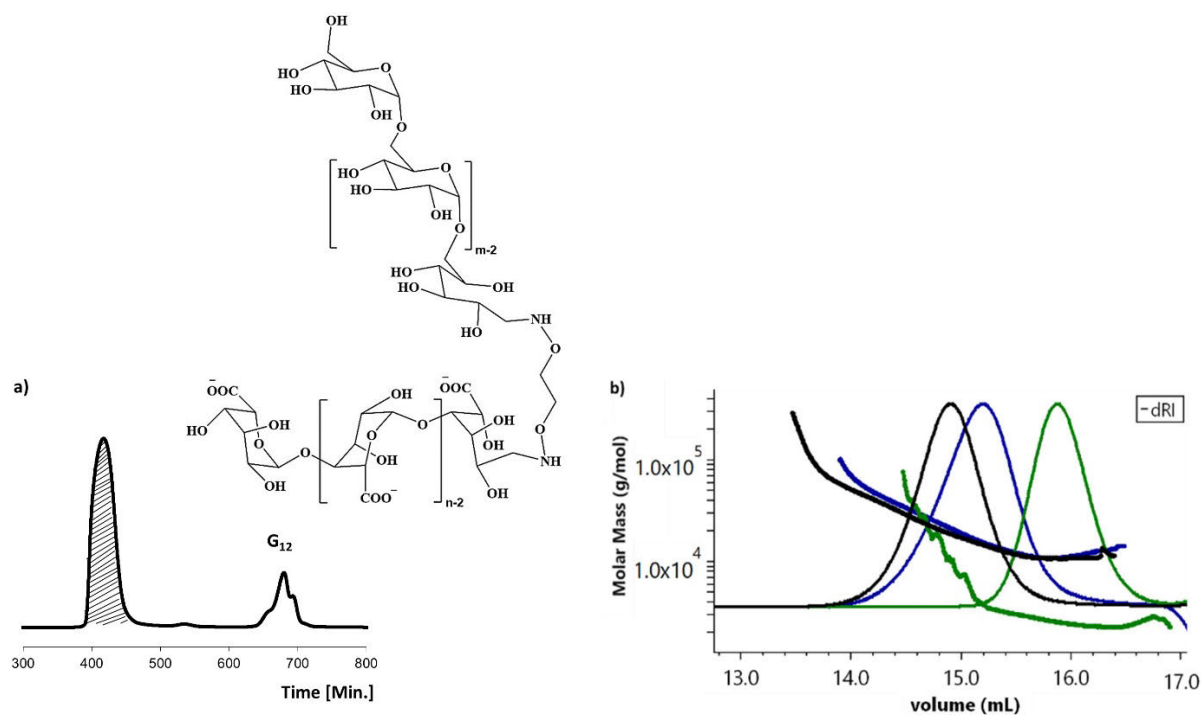


Fig. 7 G_{12} -PDHA-Dex₁₀₀ diblock polysaccharides were purified by GFC (hatched area in a) and analysed by SEC-MALS (b). The starting materials Dex₁₀₀-PDHA (blue) and G_{11} (green) were included for comparison. Molar masses are summarized in Table 6.

Table 6. M_n , M_w , and DP_n from SEC-MALS analyses of G_{12} -PDHA-Dex₁₀₀ block copolymer (after purification by GFC) and the starting material (G_{12} and Dex₁₀₀-PDHA).

Sample	M_n (kDa)	M_w (kDa)	DP_n
G_{12}	2.5	2.5	12
Dex ₁₀₀ -PDHA	16.2	18.3	100
Dex ₁₀₀ -PDHA- G_{12}	18.3	20.3	112

Calcium induced self-assembly of a G_n - b -Dex_m diblock

As a first step towards the study of the self-assembly properties of G_n -*b*-Dex_m, the solution behaviour was studied by dynamic light scattering (DLS) when CaCl₂ (20 mM) was introduced by dialysis. A membrane with a cut-off of 100 – 500 Da was used minimize the formation of out-of-equilibrium aggregates. We were initially interested in the self-assembly of the G_{40} -*b*-Dex₁₀₀ copolymer. Two relaxation modes were observed before dialysis, a fast mode corresponding to the relaxation of free chains and a slower mode corresponding to the presence of electrostatic aggregates (Fig. 8a). The scattering intensity is a good indicator of the progress of the self-assembly process. After 3 days of dialysis the intensity increased sharply and stabilized on day 7 which suggests that equilibrium or steady state had been reached (Fig. 8c). The increase in scattering intensity coincided with the disappearance of the fast mode and the transient appearance of a population with diameter around 60 nm (Fig. 8a). The final state is characterized by the presence of two populations with diameters around 25 nm and 150 nm, respectively, in the intensity size distribution. However, the second population was not detected in the number distribution (Fig. 8b), suggesting that it represented only a small fraction of the sample. The population at 25 nm probably corresponds to micellar structures consisting of an alginate-based core hydrogel stabilized by dextran blocks. The hypothesis of a core-shell morphology is supported by the fact that that G_{40} blocks alone precipitate under similar conditions. Therefore, the diblock structure enabled a strict phase separation between the G-based core and the dextran corona. Deeper characterization by small angle scattering techniques (X-ray or neutron) should allow to access the micellar characteristics in terms of radius of the core, thickness of the corona, and aggregation number. Interestingly, the G_{11} -*b*-Dex₁₀₀ diblock has a markedly different behavior under similar conditions. Initially, the scattering profiles differ. In G_{11} -*b*-Dex₁₀₀ the scattering is more dominated by the larger dextran block compared to G_{40} -*b*-Dex₁₀₀. Hence, the fast mode peak²⁷ becomes in comparison weaker. The broad peak above 100 nm also indicates some chain aggregation which disappears at the onset of the reaction since the size distribution sharpens around 100 nm and the gradually moves to higher

diameters. Large changes could however be observed upon addition of calcium. The G₁₁-*b*-Dex₁₀₀ block copolymer tended to form very large structures in solution (> 1 μ m) after a few days of dialysis (Fig. 8d). Furthermore, the scattering intensity did not increase significantly (data not shown), suggesting the formation of rather loose aggregates. From a thermodynamic point of view, this could mean that the loss of entropy associated with the formation of a dextran corona is not balanced by a sufficient gain in enthalpy through the gelling of G blocks as they are probably too short. Therefore, the ratio of the two blocks lengths must be carefully considered to have self-assembly properties in presence of calcium ions.

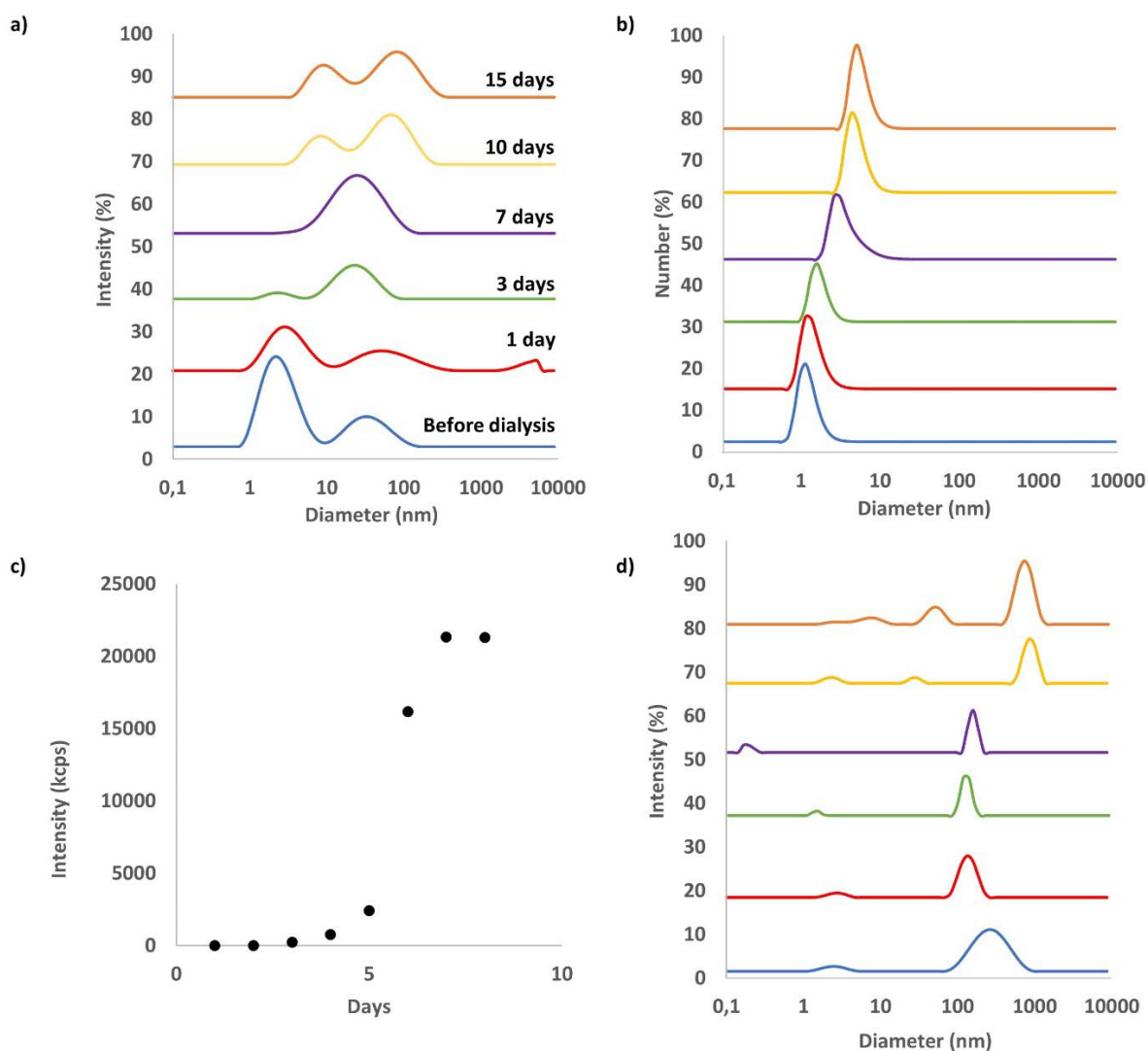


Fig. 8 Self-assembly of G_n - b -Dex₁₀₀ copolymers by dialysis (MWCO 100 – 500 Da) against Ca^{2+} (20 mM) monitored by dynamic light scattering at different timepoints. a, b) Intensity and number size distributions of G_{40} - b -Dex₁₀₀. c) Scattering intensity of G_{40} - b -Dex₁₀₀. d) Intensity size distribution of G_{11} - b -Dex₁₀₀ under similar conditions of dialysis.

Conclusions

Alginates are highly reactive towards both dihydrazides and dioxyamines, as well as with other polysaccharides that have been preactivated by such bifunctional linkers. Except for the reaction of oligomannuronates with ADH, oximes and hydrazones are stable above pH 6. All types of conjugates were readily obtained by subsequent reduction with PB. The preparation of several diblock structures with oligoguluronates (DP up to 40) based on protocols developed and optimized (detailed kinetic studies) for shorter chains was demonstrated. The flexible nature of the linker region results in a broken rod behavior of G_n -*b*- G_n diblocks in solution. Oligoguluronate-*b*-dextran diblocks were for certain chain lengths shown to form well-defined core-shell micelle-like nanoparticles by the introduction of calcium ions by dialysis, whereas free oligoguluronate chains precipitated under the same conditions. This is probably the first report of a stimuli-sensitive diblock polysaccharide without involving lateral modifications.

1. Draget, K. I.; Moe, S. T.; Skjåk-Bræk, G.; Smidsrød, O., Alginates. In *Food Polysaccharides and Their Applications*, second ed.; Stephen, A. M.; Phillips, G. O.; Williams, P. A., Eds. CRC Press: Boca Raton, 2006; pp 289-334.
2. Donati, I.; Paoletti, P., Material properties of alginates. In *Alginates: Biology and applications*, Springer-Verlag: Berlin, Heidelberg, 2009.
3. Andersen, T.; Strand, B. L.; Formo, K.; Alsberg, E.; Christensen, B. E., Alginates as biomaterials in tissue engineering. In *Carbohydrate Chemistry - Chemical and Biological Approaches*, Rauter, A. P.; Lindhorst, T. K., Eds. The Royal Society of Chemistry: Cambridge, UK, 2012; Vol. 37, pp 227-258.
4. Smidsrød, O., Molecular basis for some physical properties of alginates in the gel state. *Faraday Discussions of the Chemical Society* **1974**, 57, 263-274, 275-281.
5. Novoa-Carballal, R.; Muller, A. H. E., Synthesis of polysaccharide-*b*-PEG block copolymers by oxime click. *Chem Commun* **2012**, 48 (31), 3781-3783.
6. Bondalapati, S.; Ruvinov, E.; Kryukov, O.; Cohen, S.; Brik, A., Rapid End-Group Modification of Polysaccharides for Biomaterial Applications in Regenerative Medicine. *Macromol Rapid Comm* **2014**, 35 (20), 1754-1762.

7. Mo, I. V.; Dalheim, M. Ø.; Aachmann, F. L.; Schatz, C.; Christensen, B. E., 2, 5-Anhydro-d-Mannose End-Functionalized Chitin Oligomers Activated by Dioxyamines or Dihydrazides as Precursors of Diblock Oligosaccharides. *Biomacromolecules* **2020**, 21 (7), 2884-2895.
8. Mo, I. V.; Feng, Y.; Dalheim, M. Ø.; Solberg, A.; Aachmann, F. L.; Schatz, C.; Christensen, B. E., Activation of enzymatically produced chitoooligosaccharides by dioxyamines and dihydrazides. *Carbohydrate Polymers* **2020**, 232, 115748.
9. Smidsrød, O.; Haug, A., Dependence upon uronic acid composition of some ion-exchange properties of alginates. *Acta Chemica Scandinavica* **1968**, 22, 1989-1997.
10. Nordgård, C. T.; Draget, K. I., Oligosaccharides as modulators of rheology in complex mucous systems. *Biomacromolecules* **2011**, 12 (8), 3084-3090.
11. Gimmetstad, M.; Sletta, H.; Ertesvåg, H.; Bakkevig, K.; Jain, S.; Suh, S.-j.; Skjåk-Bræk, G.; Ellingsen, T. E.; Ohman, D. E.; Valla, S., The *Pseudomonas fluorescens* AlgG protein, but not its mannuronan C-5-epimerase activity, is needed for alginate polymer formation. *Journal of bacteriology* **2003**, 185 (12), 3515-3523.
12. Ertesvåg, H.; Skjåk-Bræk, G., Modification of alginate using mannuronan C-5-epimerases. In *Carbohydrate biotechnology protocols*, Springer: 1999; pp 71-78.
13. Baudendistel, O. R.; Wieland, D. E.; Schmidt, M. S.; Wittmann, V., Real-Time NMR Studies of Oxyamine Ligations of Reducing Carbohydrates under Equilibrium Conditions. *Chemistry—A European Journal* **2016**, 22 (48), 17359-17365.
14. Paulo, E. M.; Boffo, E. F.; Branco, A.; Valente, Â. M.; Melo, I. S.; Ferreira, A. G.; Roque, M. R.; Assis, S. A. d., Production, extraction and characterization of exopolysaccharides produced by the native *Leuconostoc pseudomesenteroides* R2 strain. *Anais da Academia Brasileira de Ciências* **2012**, 84 (2), 495-508.
15. Cheetham, N. W.; Slodki, M. E.; Walker, G. J., Structure of the linear, low molecular weight dextran synthesized by a D-glucosyltransferase (GTF-S3) of *Streptococcus sobrinus*. *Carbohydrate polymers* **1991**, 16 (4), 341-353.
16. van Dijk-Wolthuis, W.; Franssen, O.; Talsma, H.; Van Steenbergen, M.; Kettenes-Van Den Bosch, J.; Hennink, W., Synthesis, characterization, and polymerization of glycidyl methacrylate derivatized dextran. *Macromolecules* **1995**, 28 (18), 6317-6322.
17. Haug, A.; Larsen, B. In *A study on the constitution of alginic acid by partial acid hydrolysis*, Proceedings of the Fifth International Seaweed Symposium, Halifax, August 25–28, 1965, Elsevier: 1966; pp 271-277.
18. Haug, A.; Larsen, B.; Smidsrød, O., Studies on the sequence of uronic acid residues in alginic acid. *Acta chem. scand* **1967**, 21 (3), 691-704.
19. Holtan, S.; Zhang, Q.; Strand, W. I.; Skjåk-Bræk, G., Characterization of the hydrolysis mechanism of polyalternating alginate in weak acid and assignment of the resulting MG-oligosaccharides by NMR spectroscopy and ESI– mass spectrometry. *Biomacromolecules* **2006**, 7 (7), 2108-2121.

20. Haug, A., Composition and properties of alginates. **1964**.
21. Kwase, Y. A.; Cochran, M.; Nitz, M., Protecting-Group-Free Glycoconjugate Synthesis: Hydrazide and Oxyamine Derivatives in N-Glycoside Formation. In *Modern synthetic methods in carbohydrate chemistry: From monosaccharides to complex glycoconjugates*, Werz, D. B.; Vidal, S., Eds. Wiley: 2013; pp 67-96.
22. Spiro, M. D.; Ridley, B. L.; Glushka, J.; Darvill, A. G.; Albersheim, P., Synthesis and characterization of tyramine-derivatized (1→4)-linked alpha-D-oligogalacturonides. *Carbohydr Res* **1996**, 290 (2), 147-57.
23. Vold, I. M. N.; Kristiansen, K. A.; Christensen, B. E., A study of the chain stiffness and extension of alginates, in vitro epimerized alginates, and periodate-oxidized alginates using size-exclusion chromatography combined with light scattering and viscosity detectors. *Biomacromolecules* **2006**, 7, 2136-2146.
24. Smidsrød, O.; Glover, R. a.; Whittington, S. G., The relative extension of alginates having different chemical composition. *Carbohydrate research* **1973**, 27 (1), 107-118.
25. Yuguchi, Y.; Hasegawa, A.; Padol, A. M.; Draget, K. I.; Stokke, B. T., Local structure of Ca²⁺ induced hydrogels of alginate-oligoguluronate blends determined by small-angle-X-ray scattering. *Carbohydrate Polymers* **2016**, 152, 532-540.
26. Nakauma, M.; Funami, T.; Fang, Y. P.; Nishinari, K.; Draget, K. I.; Phillips, G. O., Calcium binding and calcium-induced gelation of sodium alginate modified by low molecular-weight polyuronate. *Food Hydrocolloid* **2016**, 55, 65-76.
27. Sedlák, M., What can be seen by static and dynamic light scattering in polyelectrolyte solutions and mixtures? *Langmuir* **1999**, 15 (12), 4045-4051.

Supporting Information

Alginate-based diblock polymers: Preparation, characterization and Ca-induced self-assembly

Amalie Solberg[†], Ingrid V. Mo[†], Finn L. Aachmann[†], Christophe Schatz[‡] and Bjørn E. Christensen^{†}*

[†]NOBIPOL, Department of Biotechnology and Food Science, NTNU Norwegian University of Science and Technology, Sem Sælands vei 6/8, NO-7491 Trondheim, Norway

[‡]LCPO, Université de Bordeaux, UMR 5629, ENSCBP, 16, Avenue Pey Berland, 33607 Pessac Cedex, France

Contents

Preparation and characterization of guluronate oligomers (G_n)	2
Conjugation with PDHA	4
Conjugation with ADH	13
Attachment of the second block: A-<i>b</i>-B diblock polysaccharides	16
Reduction of oximes/hydrazones/N-pyranosides with α-picoline borane	19
References	26

Preparation and characterization of guluronate oligomers (G_n)

Pure guluronate oligomers (G_n) were prepared by acid precipitation of guluronate rich alginates, removing any oligomers containing one or more M-residue(s).

A study using high-performance anion-exchange chromatography with pulsed amperometric detection (HPAEC-PAD) was performed, monitoring the acid hydrolysis of a guluronate with DP_n 20, enabling tailoring of the resulting DP_n .

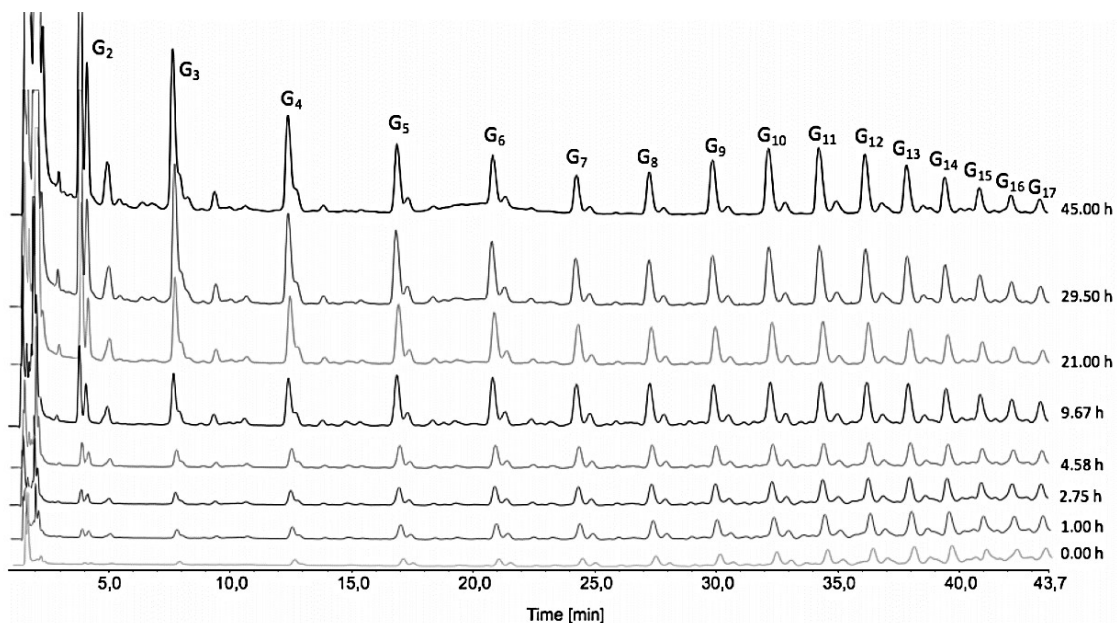


Fig. S1 HPAEC-PADH chromatograms for guluronate oligomers taken at different timepoints during hydrolysis (95°C, pH 3.62).

Oligomers with defined DP_n were prepared by GFC, and DP_n was verified by 1H -NMR (Fig. S3). Isolated triguluronate was annotated according to literature¹.

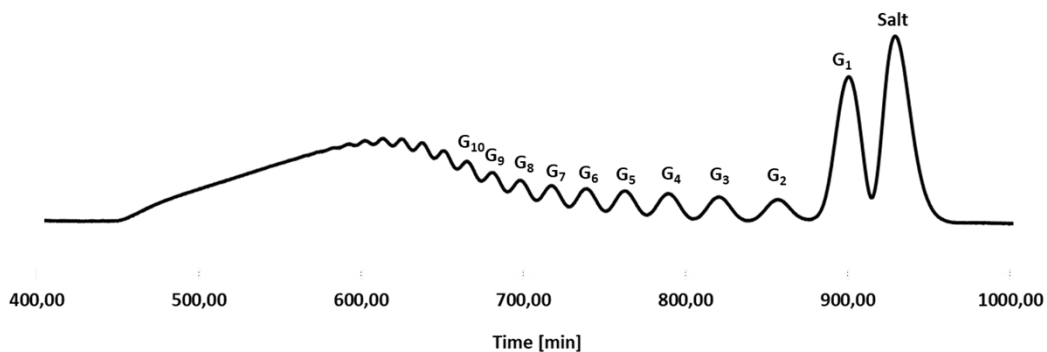


Fig. S2 GFC fractionation of guluronate oligomers (guluronate with DPn 20 hydrolyzed for 9 h at 95°, pH 3.61).

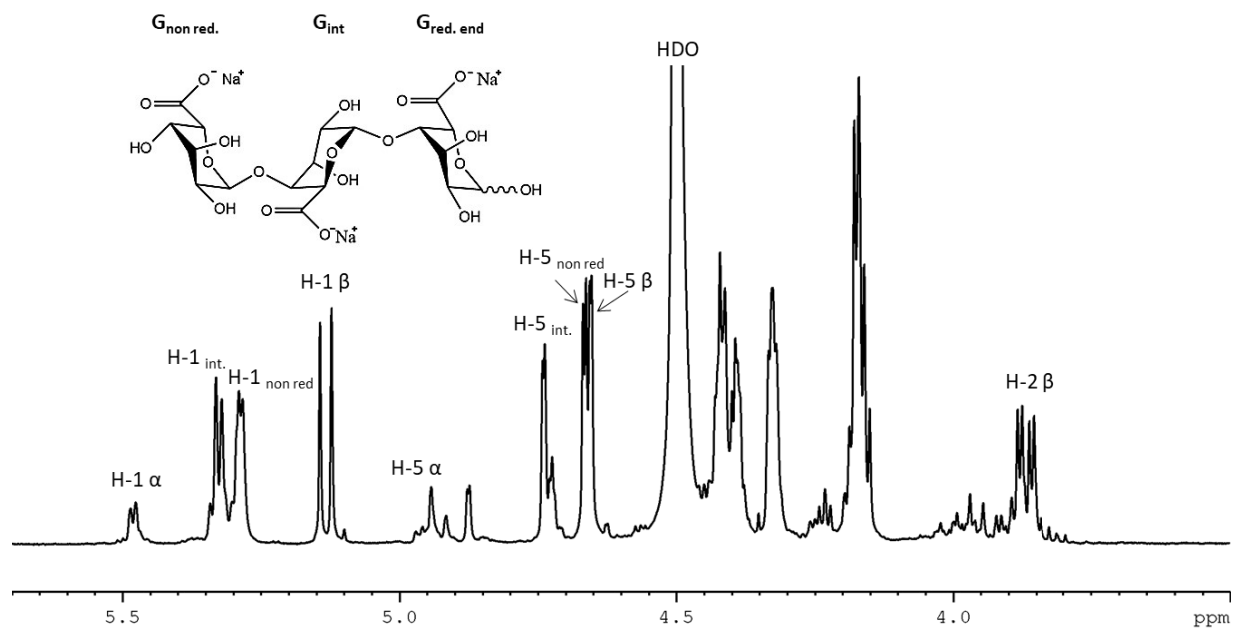


Fig. S3 $^1\text{H-NMR}$ (82 °C, 400 MHz) spectrum of isolated triguluronate, peaks were assigned according to literature ¹.

Conjugation with PDHA

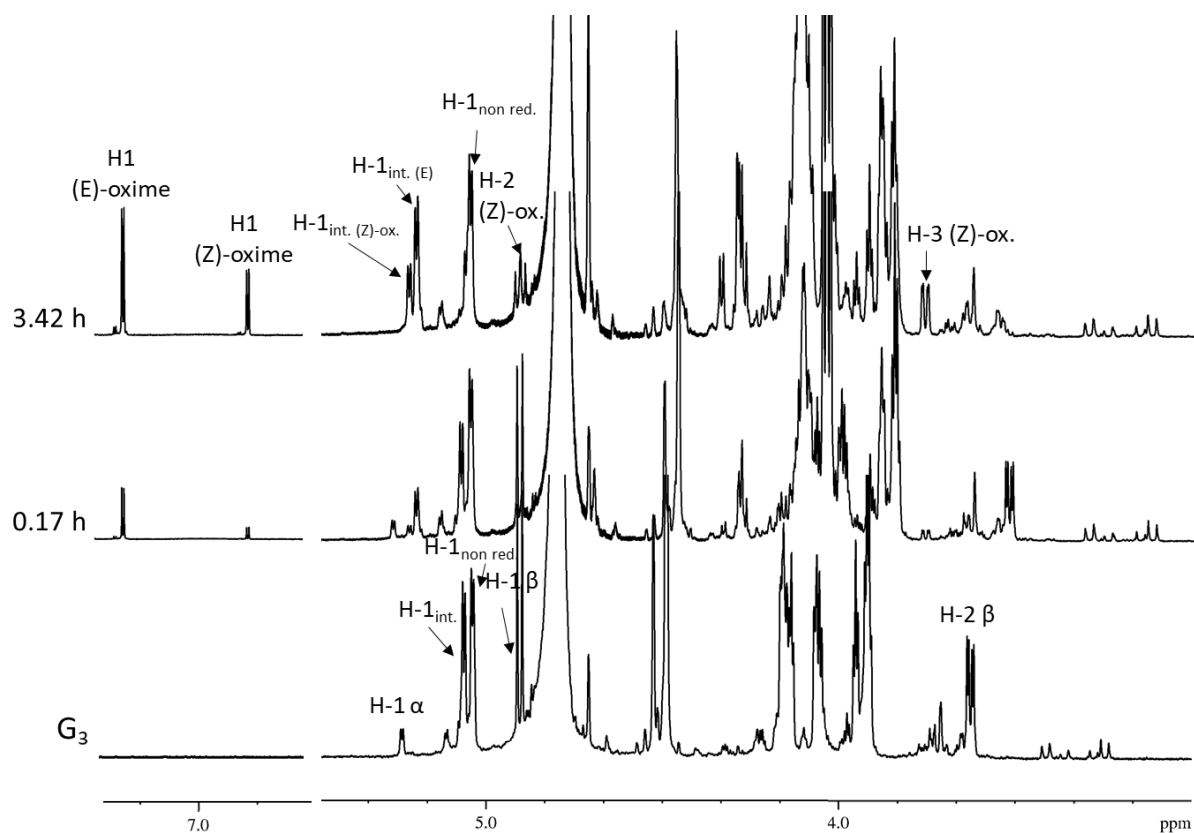


Fig. S4 Stack of ¹H-NMR spectra obtained after different timepoints for the reaction with G₃ (7mM) and PDHA (2 equiv.) in 500 mM AcOH[d₄] pD 4 (27 °C, 600 MHz). Pure G₃ (in buffer) is included for comparison.

The equilibrium reaction mixture with G₃ and PDHA was characterized by heteronuclear NMR.

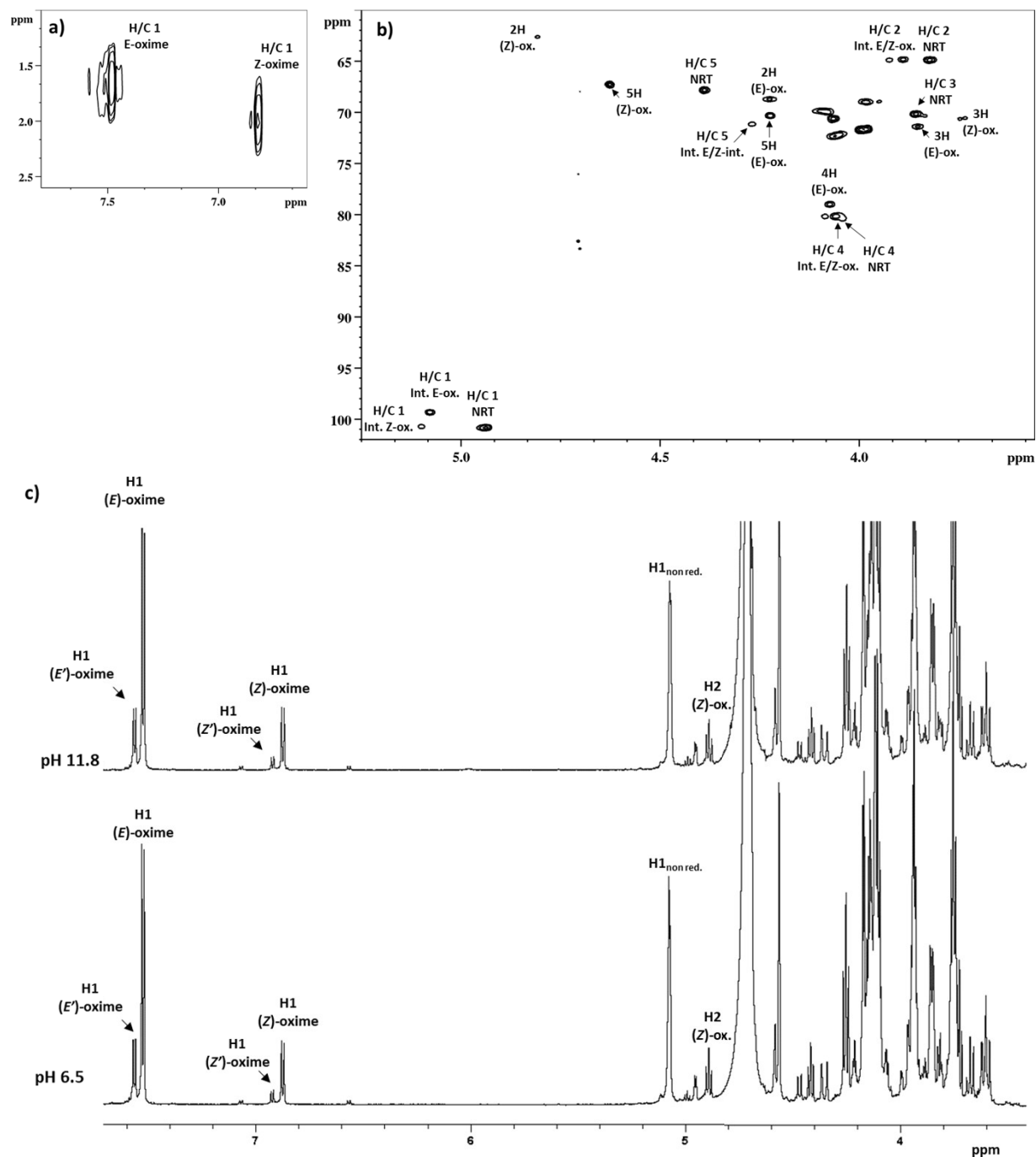


Fig. S5 a,b) ¹³C HSQC of the reaction mixture obtained for the conjugation with G₃ (7mM) and PDHA (2 equiv.) (500 mM AcOH[d₄] pD 4) recorded at t > 24 h (82 °C, NEO 600 MHz magnet). c) ¹H-NMR spectra of G₃-PDHA after purification by GFC and dialysis in D₂O at pH 6.5 and 11.8 (27 °C, 600 MHz)

Table S1: Assignment of chemical shifts for the reaction mixture with G ₃ and PDHA obtained from HSQC, h2BC and HMBC (G ₃ (7mM) and PDHA (14 mM) in 500 mM AcOH[d4] pD 4) (82 °C, NEO 600 MHz)						
	H1/C1	H2/C2	H3/C3	H4/C4	H5/C5	C6
(E)-oxime	7.48; 151.5	4.23; 68.6	3.86; 71.38	4.07; 79.0	4.22; 70.3	177.1
(Z)-oxime	6.83; 152.0	4.81; 62.63	3.74; 70.65	4.03; 80.35	4.27; 71.24	175.2
Int. (E)-oxime	5.07; 99.22	3.89; 64.86	3.97; 68.92	4.08; 79.0	4.27; 71.16	177.1
Int. (Z)-oxime	5.09; 100.5	3.92; 64.89	3.99; 68.92	4.04; 80.42	4.27; 71.16	177.1
NRT	4.94; 100.77	3.82; 70.19	3.86; 70.65	4.07; 80.2	4.39; 67.8	175.2

The reaction kinetics was determined by integrating the ¹H-NMR spectra, using H1 of the non-reducing end and TSP as internal standards. A simple model based on first order kinetics was used to determine the rate constants (k_T and k_{-T}) for the combined yield.

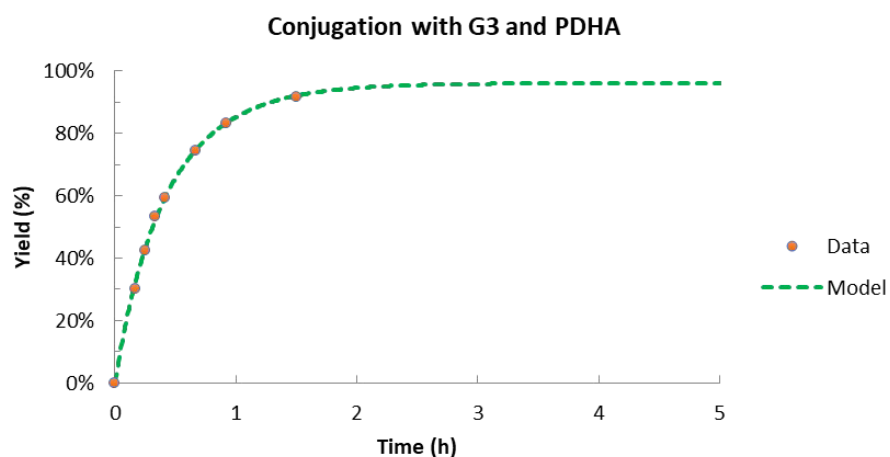


Fig. S6 Conjugation with G₃ (7mM) and PDHA (2 equiv.) (500 mM AcOHd4 pD 4) studied by time course NMR (27 °C, 600 MHz). Data obtained by integration using ¹H of the non-reducing ends as internal standard. A simple model assuming first order kinetics based on combined yield is included.

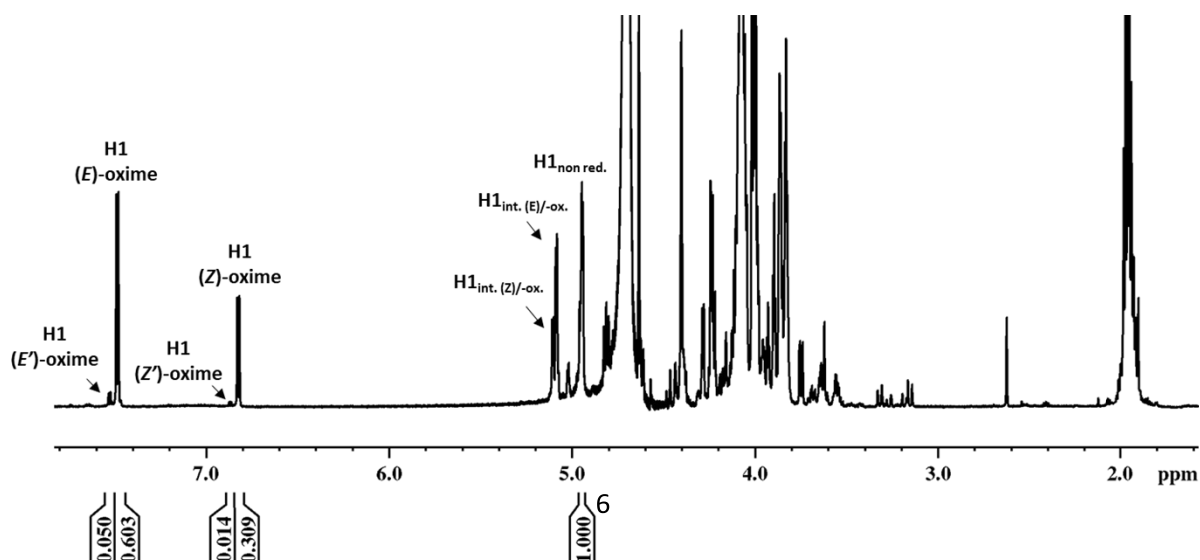


Fig. S7 ^1H -NMR spectra of the equilibrium reaction mixture with G_3 (7mM) and PDHA (2 equiv.) (in 500 mM AcOHd_4 pD 4 at 27 $^\circ\text{C}$, 600 MHz) recorded after 4 h. Integration using H1 of the non-reducing end used to estimate yield is included.

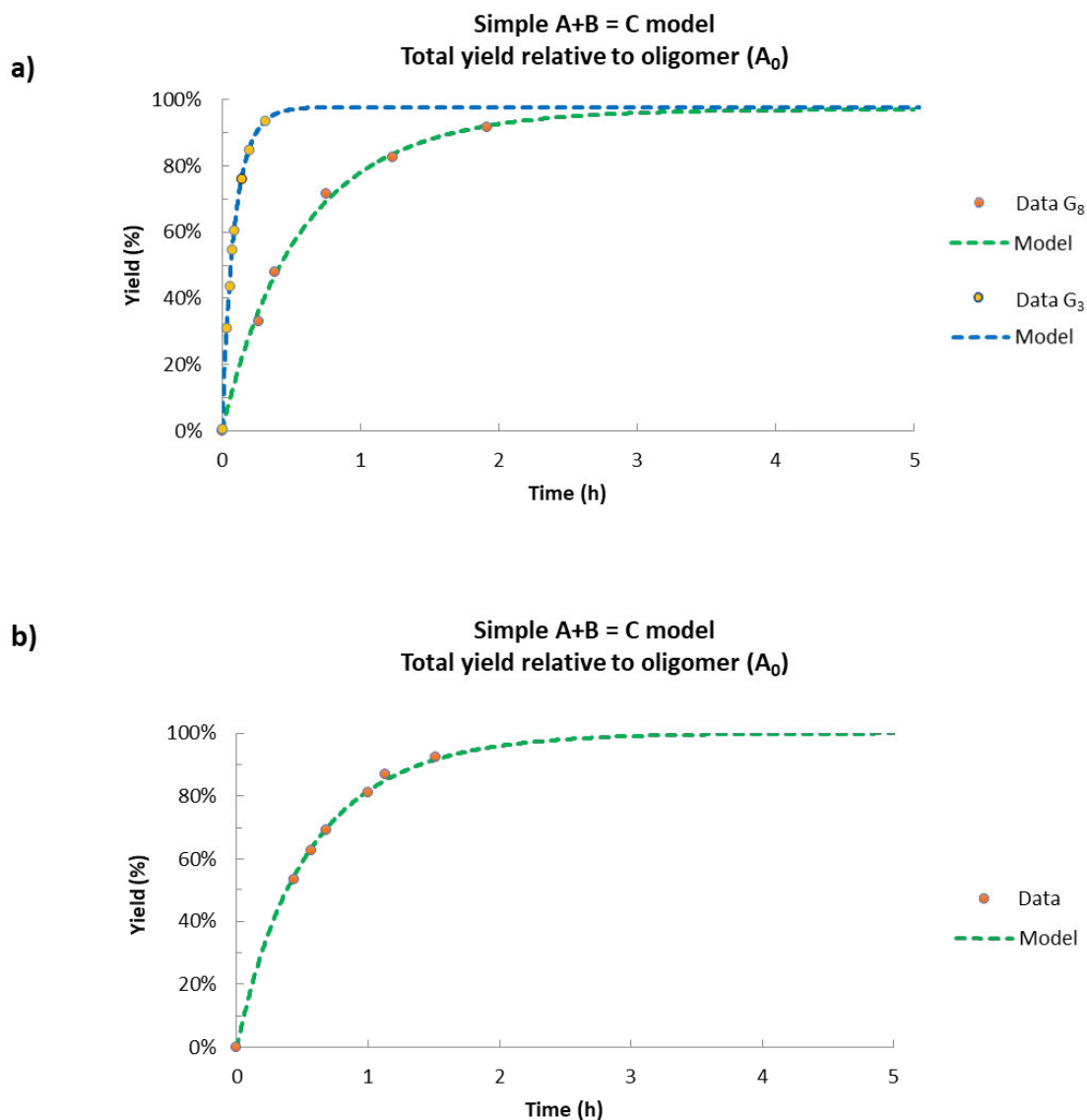


Fig. S8 Plot with combined yield for conjugation with a) G_8 (7mM) and b) G_6 (20 mM) and PDHA (2 equiv.) (500 mM AcOHd_4 pD 4) studied by time course NMR. Data obtained by integration using H1 of the non-reducing ends as internal standard. A simple model assuming first order kinetics based on combined yield is included.

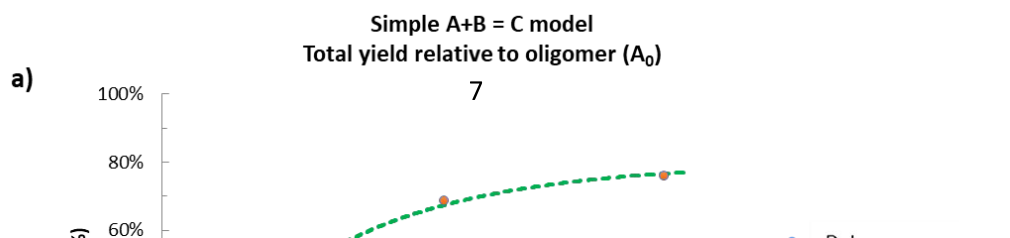


Fig. S9 Plot with combined yield for conjugation with a) Dextran DP 3 (7mM) and b) Maltotriose (7 mM) and PDHA (2 equiv.) (500 mM AcOHd4 pD 4) studied by time course NMR (27 °C, 600 MHz). Data obtained by integration using H1 of the non-reducing ends or TSP as internal standard. A simple model assuming first order kinetics based on combined yield is included.

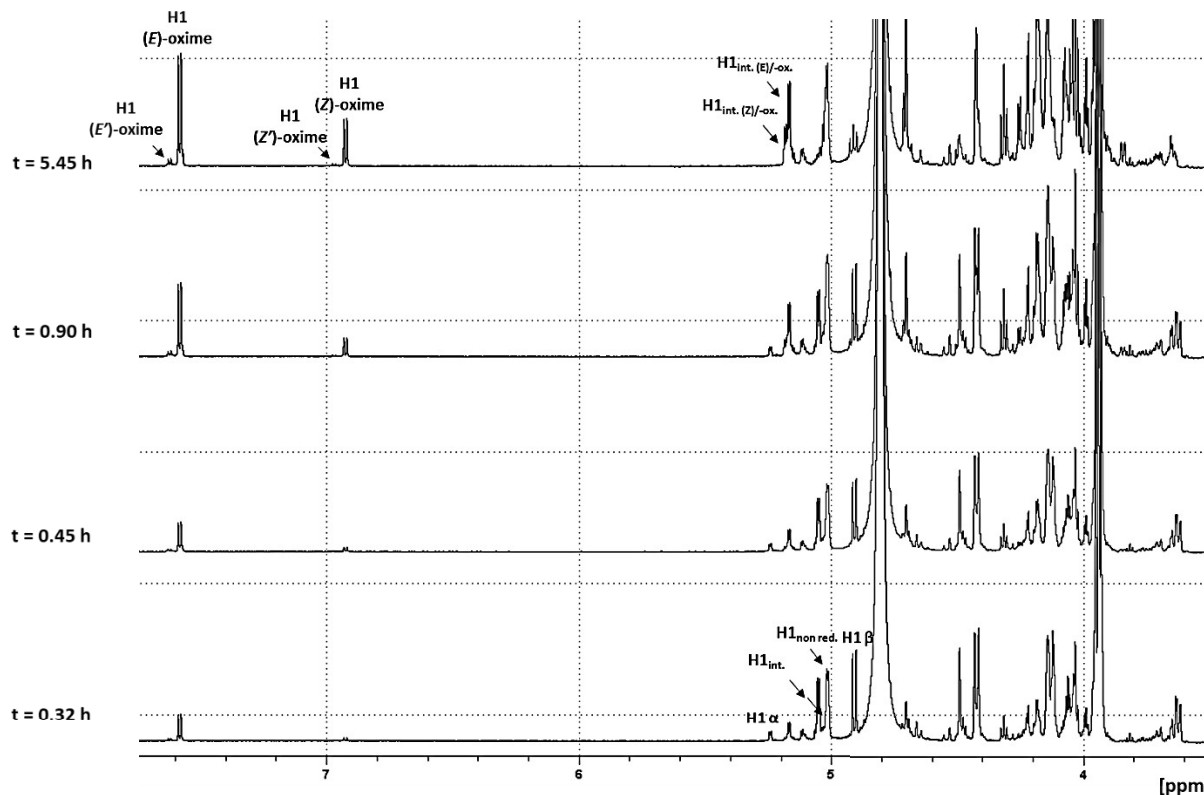


Fig. S10 Stack of ¹H-NMR spectra obtained at different time points for the reaction with G₃ (7mM) and PDHA (2 equiv.) at pD 5 (500 mM AcOHd4, 27 °C, 600 MHz).

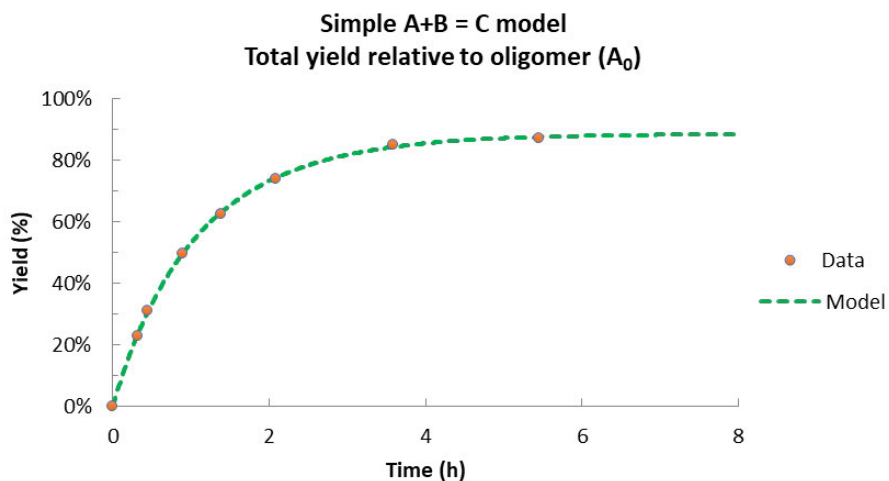


Fig. S11 Conjugation with G₃ (7mM) and PDHA (2 equiv.) at pD 5 (500 mM AcOHd4) studied by time

course NMR (obtained at 27 °C, using a 600 MHz magnet). Data obtained by integration using H1 of the non-reducing ends as internal standard. A simple model assuming first order kinetics based on combined yield is included.

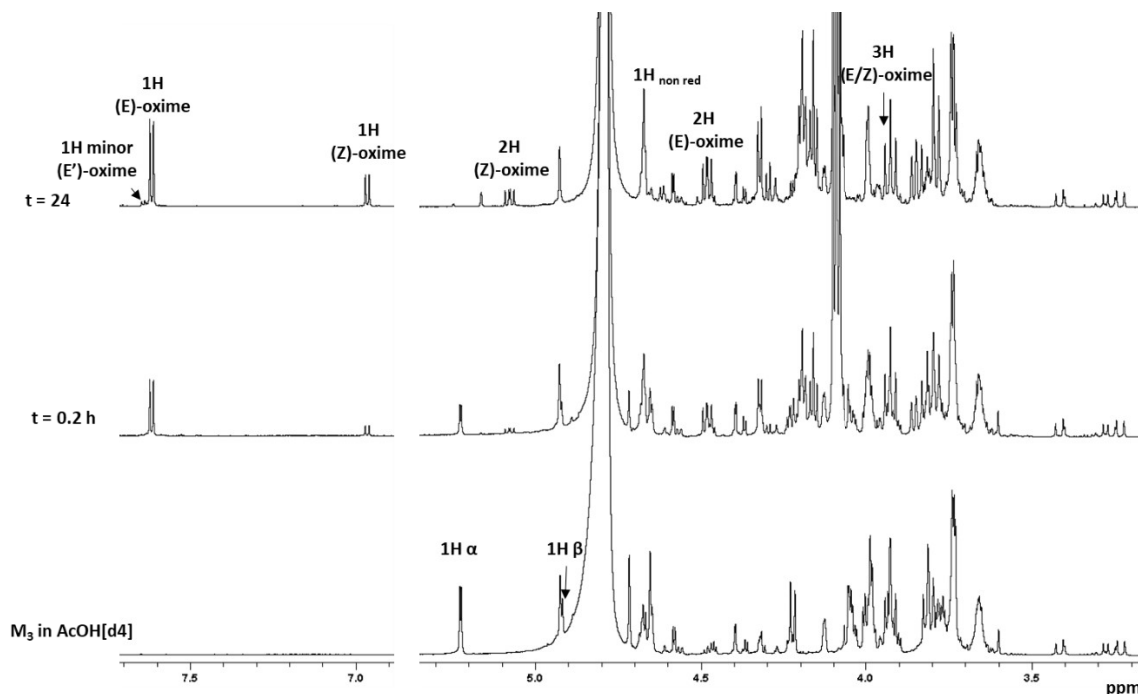


Fig. S12 Stack of 1D ¹H-NMR spectra obtained at different timepoints for the reaction with M₃ (7mM) and PDHA (2 equiv.) in 500 mM AcOH[d₄] (27 °C, 600 MHz) (M₃ is included for comparison). Key resonances indicative of the reaction are annotated.

The reaction mixture with M₃ and PDHA (24 h reaction time, 10 equiv. PDHA, 500 mM NaAc-buffer pH 4) was purified by GFC, dialysis and freeze drying.

H1 of the oxime conjugates were assigned based on literature^{2,3}. H2 and H3 of the (E)- and (Z)-oxime was assigned using 1D selective COSY and TOCY NMR (Fig. S13). Complete assignment was obtained by heteronuclear NMR, Fig. S14.

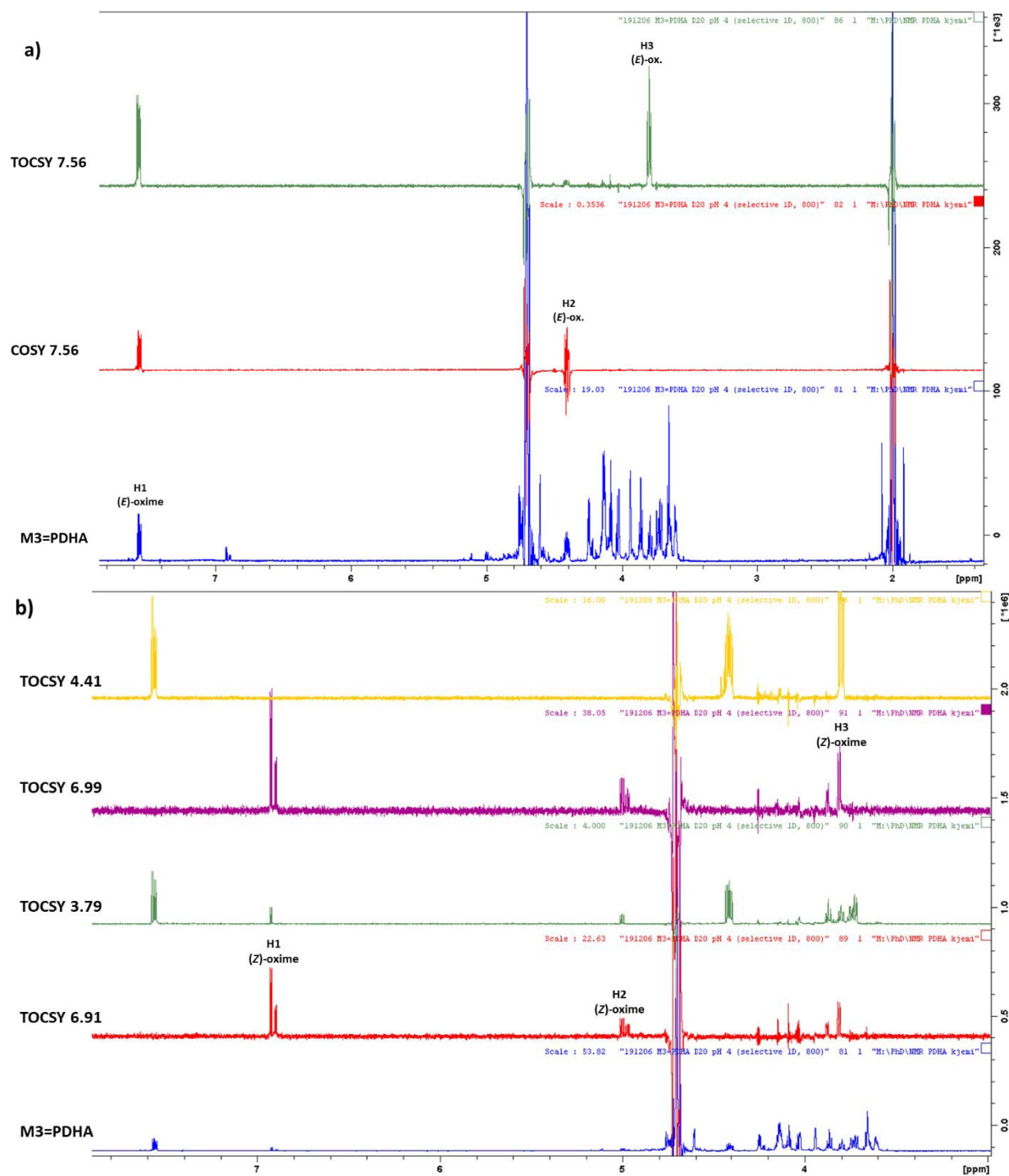


Fig. S13 1D selective COSY and TOCSY NMR spectra of M₃-PDHA (after purification) in D₂O, pH 4 (25 °C, 800 MHz). a) Assignment of H1-H3 of the (E)-oxime, and b) assignment of H1-H3 of the (Z)-oxime. The ppm of the pulse is indicated to the left.

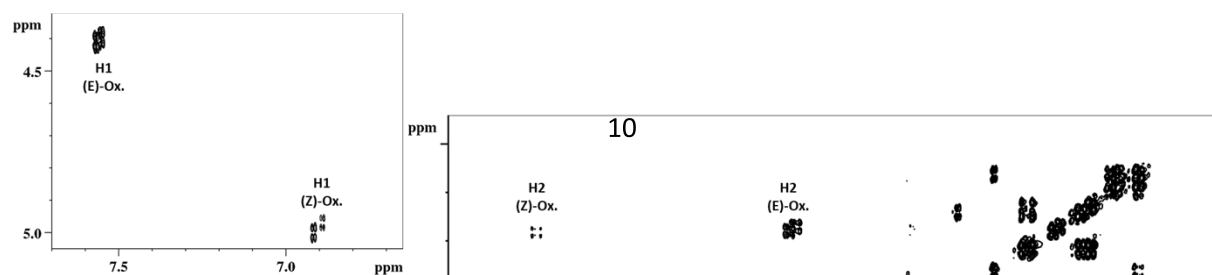


Fig. S14 ^1H - ^1H COSY spectra of the oxyamine modified trimannuronate (M_3 -PDHA) (after purification by GFC, dialysis and freeze drying) in D_2O pH 4 (25 °C, 800 MHz).

Table S2: Assignment of chemical shifts for oxyamine modified trimannuronate (M_3 -PDHA) (after purification by GFC, dialysis and freeze drying) in D_2O pH 4 obtained from 1D selective and heteronuclear NMR experiments. Prime indicates the minor form.							
	H/C 1	H/C 1'	H/C 2	H/C 3	H/C 4	H/C 5	C 6
(E)-oxime	7.61; 151.7	7.65; 151.7	4.40; 68.04	3.79; 75.65	4.11; 77.6	4.25; 71.31	178.1
(Z)-oxime	6.96; 151.6	7.00; 151.3	4.98; 63.1	3.79; 75.65	4.11; 77.6	4.25; 71.31	178.1

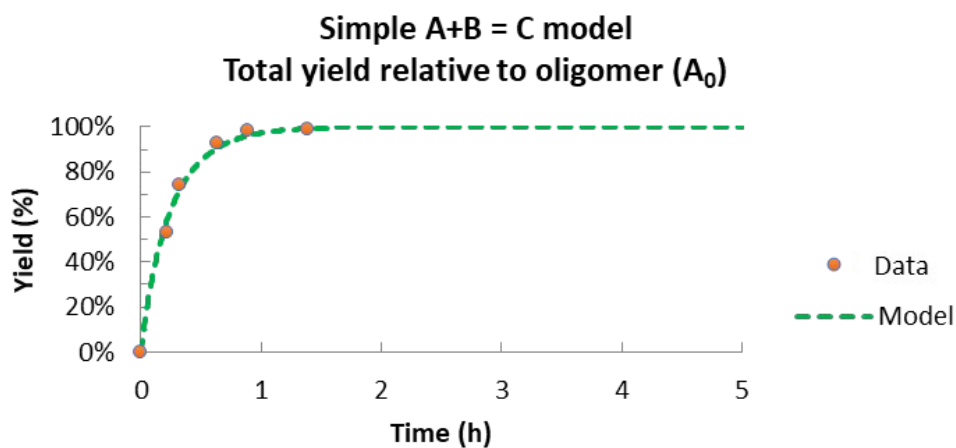


Fig. S15 Plot with combined yield for conjugation with M_3 (7 mM) and PDHA (2 equiv.) (500 mM AcOHd4 pD 4) studied by time course NMR (at 27 °C using the 600 MHz). Data obtained by integration using TSP as internal standard. A simple model assuming first order kinetics based on combined yield is included.

Conjugation with ADH

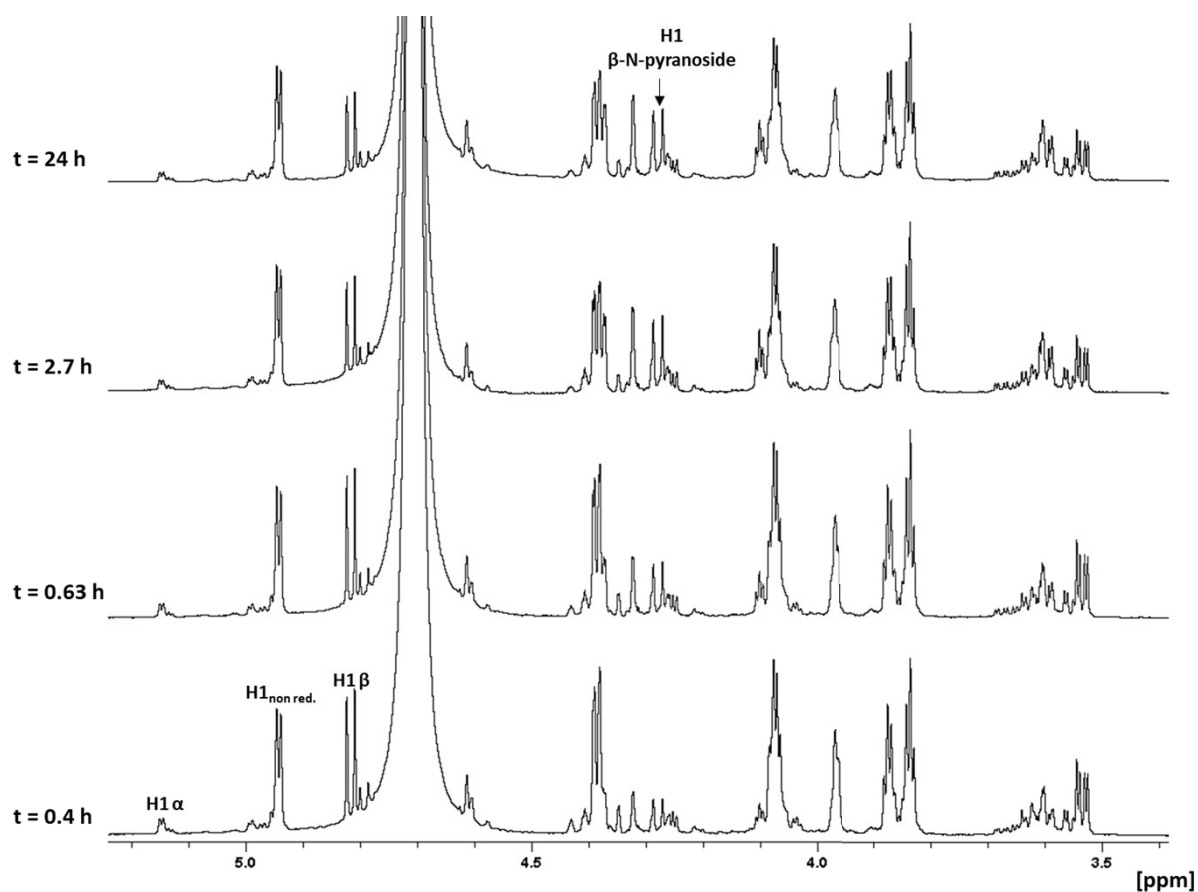


Fig. S16 Stack of ^1H -NMR spectra (27 °C, 600 MHz) obtained at different time points for the reaction with G_2 (7mM) and ADH (2 equiv.) at pD 4 (500 mM AcOHd_4).

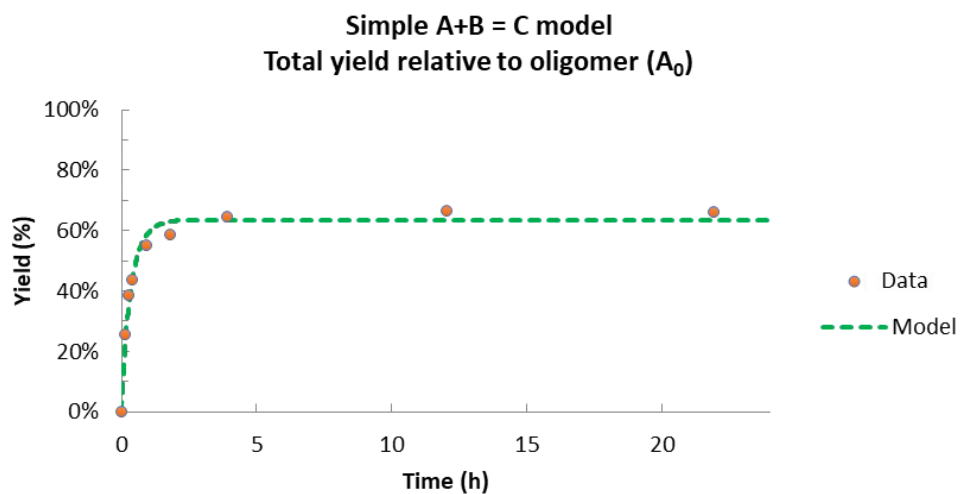


Fig. S17 Plot with combined yield for conjugation with G_2 (7 mM) and ADH (2 equiv.) (500 mM AcOHd4 pD 4) studied by time course NMR (at 27 °C using a 600 MHz magnet). Data obtained by integration using H1 of the non-reducing end as internal standard. A simple model assuming first order kinetics based on combined yield is included.

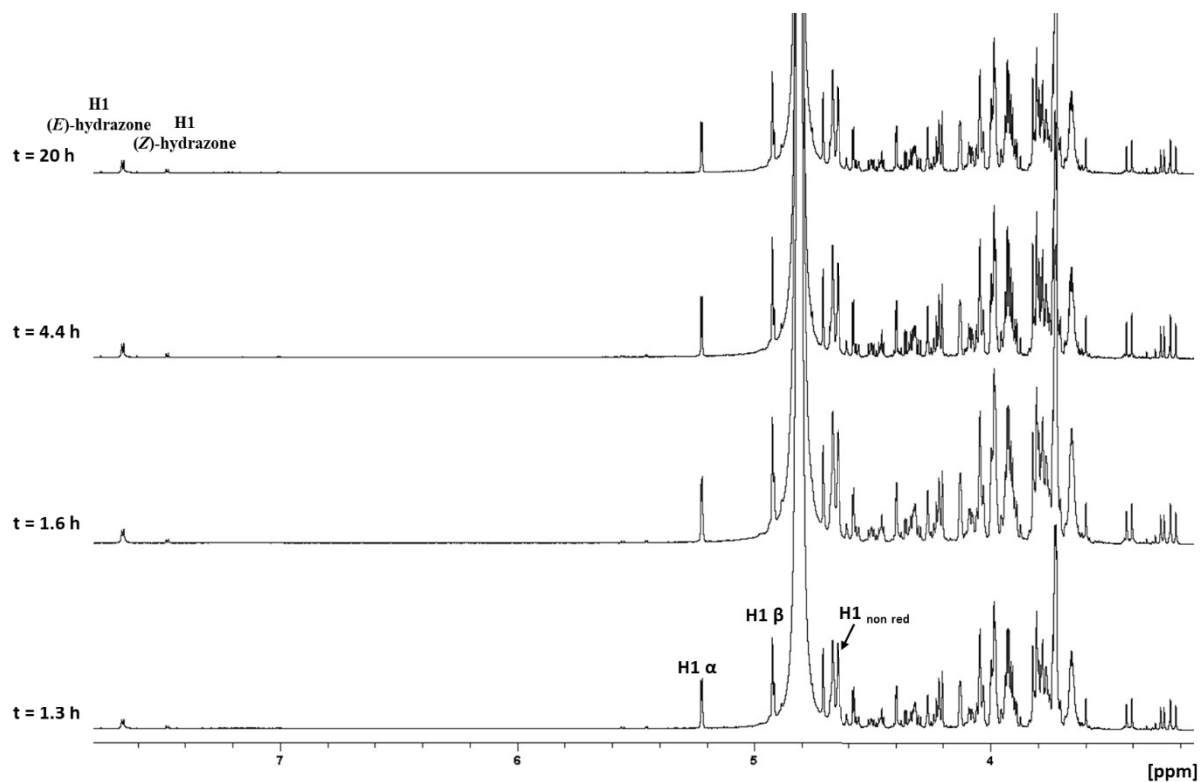


Fig. S18 Stack of ^1H -NMR (27 °C, 600 MHz) spectra obtained at different time points for the reaction with M_3 (7mM) and ADH (2 equiv.) at pD 4 (500 mM AcOHd_4).

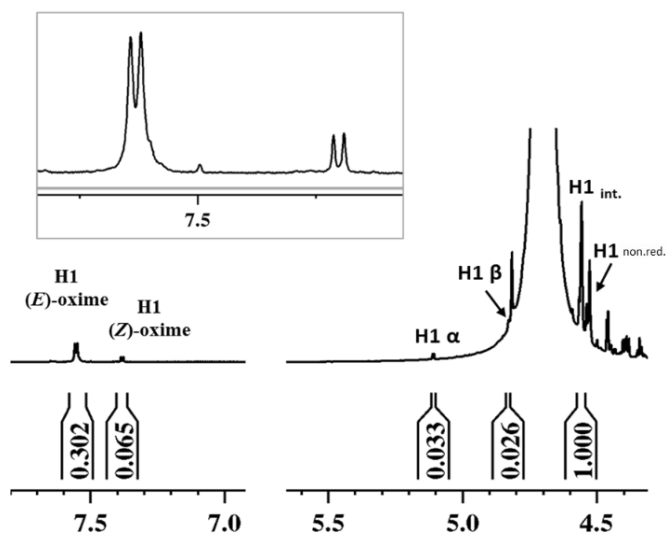


Fig. S19 ^1H -NMR (27 °C, 600 MHz) spectrum of the equilibrium reaction mixture ($t > 20$ h) for the reaction with M_3 (7mM) and ADH (10 equiv.) (500 mM AcOHd_4 pD 4).

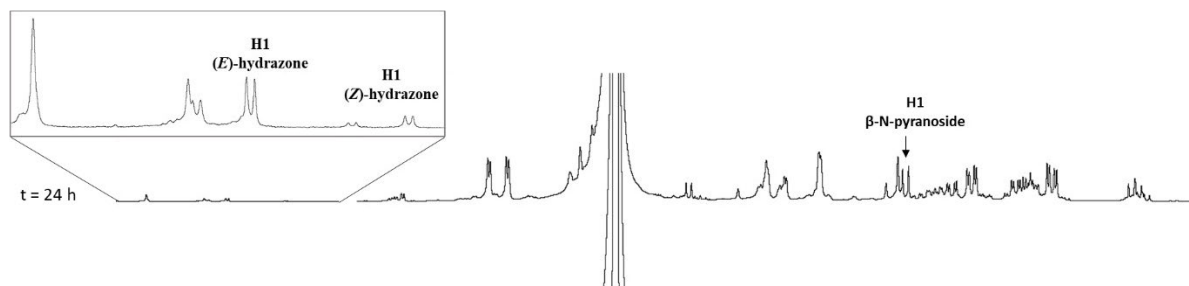


Fig. S20 Stack of ^1H -NMR (27 °C, 600 MHz) spectra obtained at different time points for the reaction with Galacturonic acid DP 3 (TriGalA_3) (7mM) and ADH (2 equiv.) at pD 4 (500 mM AcOHd_4). A spectrum of pure TriGalA is included for comparison.

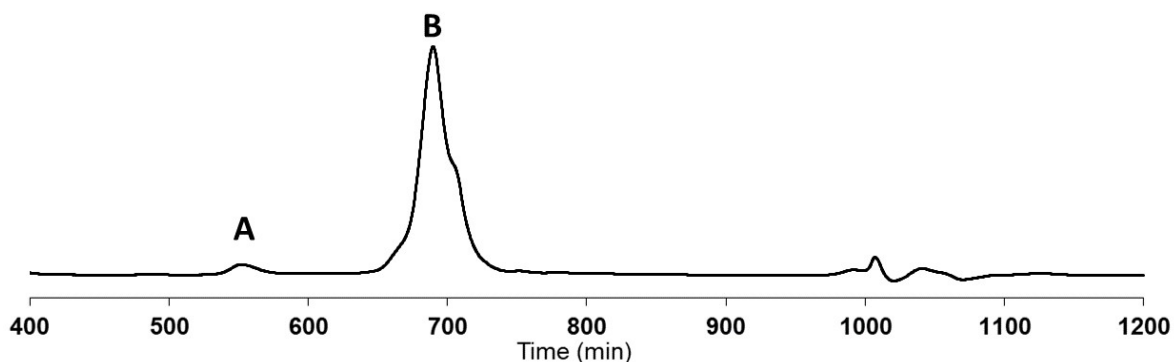


Fig. S21 GFC fractions of the products formed in the reaction with G_{10} and PDHA (10 equiv.) with PB (3 equiv.).

Product having elution times corresponding to peak B (Fig. S21) is in agreement with G_{10} -PDHA. Peak A has elution volumes corresponding to a G_{10} -PDHA- G_{10} based on comparison to a G_n hydrolysate.

Attachment of the second block: A-*b*-B diblock polysaccharides

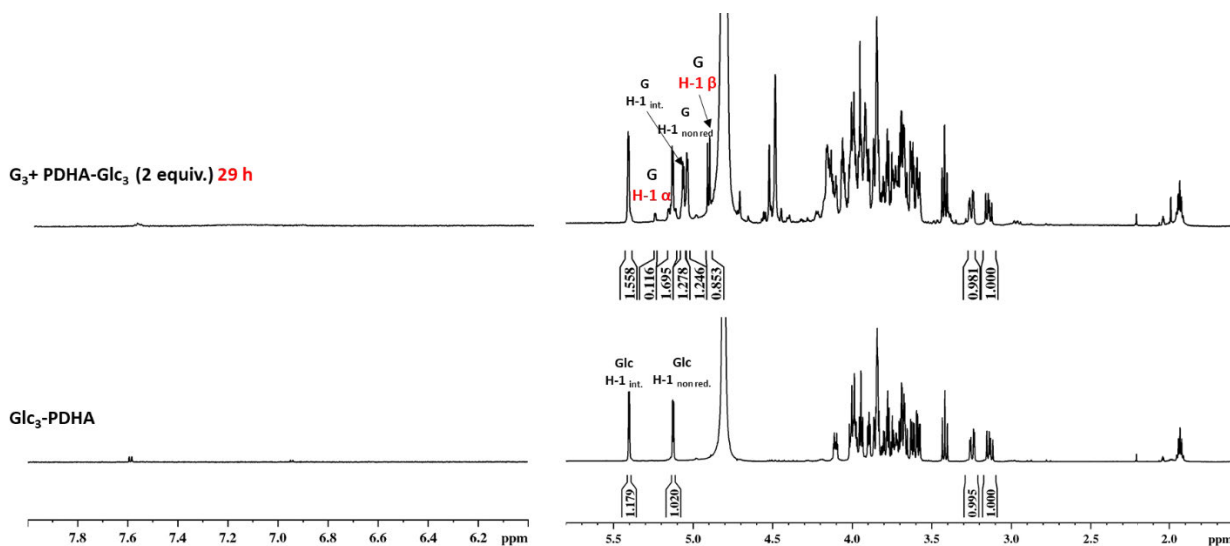


Fig. S22 ^1H -NMR (27 °C, 600 MHz) spectrum of the reaction mixture with G_3 (7mM) and maltotriose DP 3 with PDHA (Glc_3 -PDHA) (2 equiv.) (500 mM AcOHd_4 pD 4). Purified Glc_3 -PDHA (in 500 mM AcOHd_4 pD 4) is included for comparison.

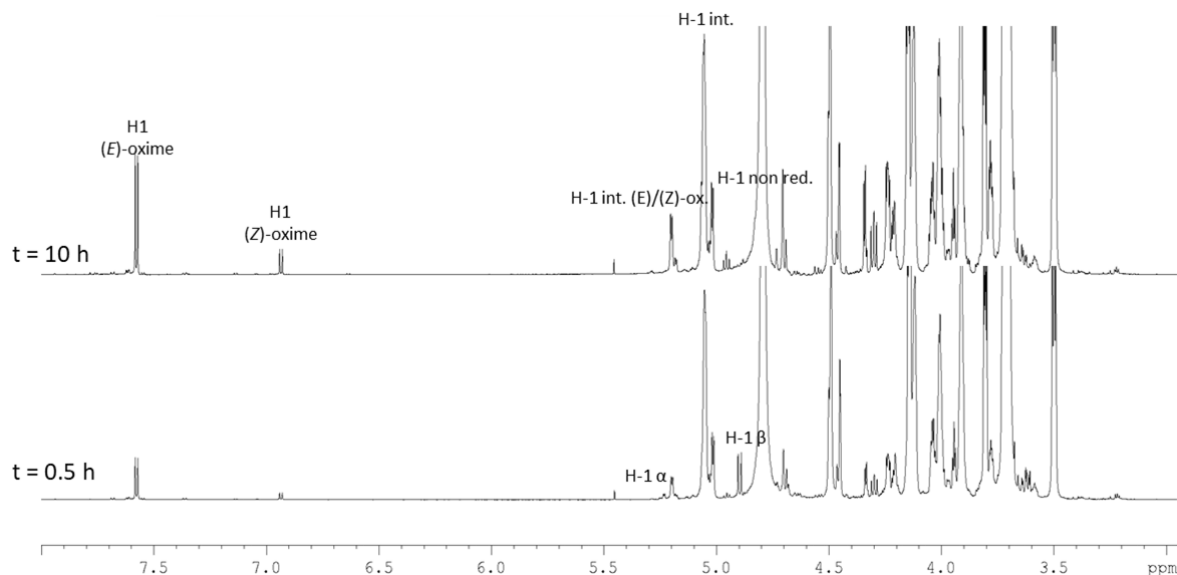


Fig. S23 Stack of ^1H -NMR (27 °C, 600 MHz) spectra obtained at different time points for the reaction with G_7 (20.1 mM) and aminoox- $\text{PEG}_5\text{-N}_3$ (2 equiv.) (500 mM AcOHd_4 , pD 4).

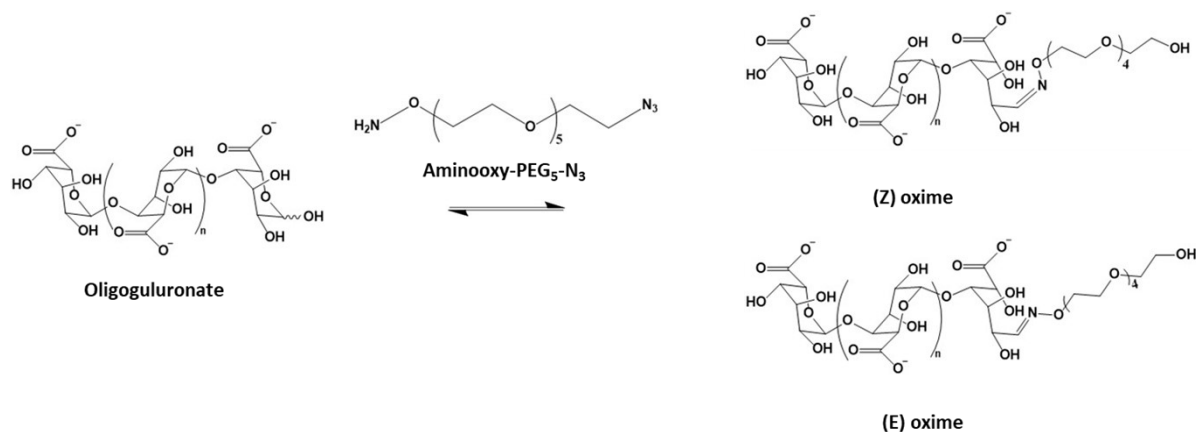


Fig. S24 Reaction scheme for the reaction with G_7 and aminoox- $\text{PEG}_5\text{-N}_3$.

Reduction of oximes/hydrazones/N-pyranosides with α -picoline borane

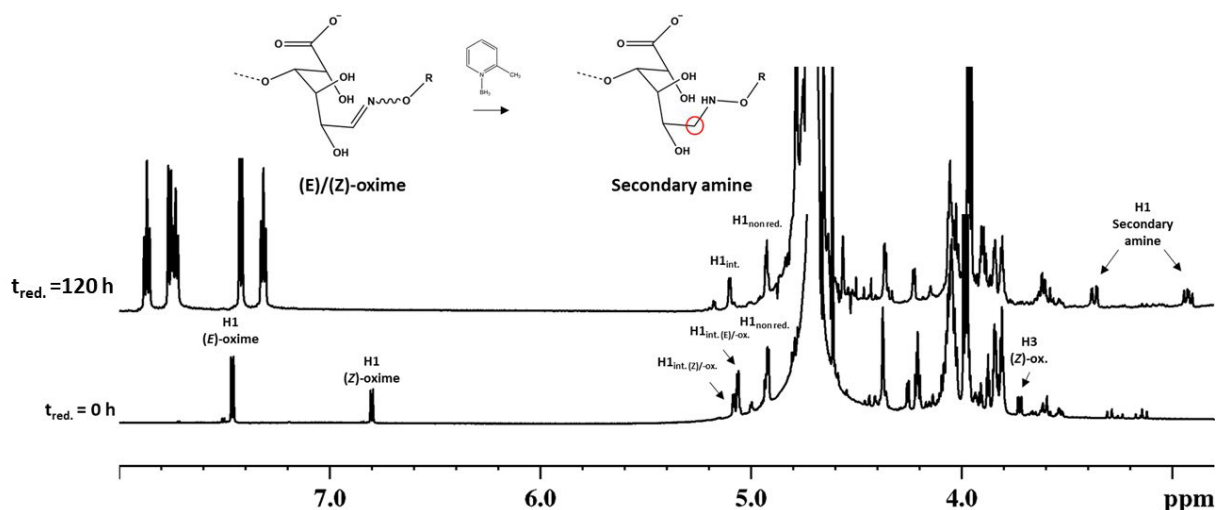


Fig. S25 ^1H -NMR (27 °C, 600 MHz) spectra of equilibrium reaction mixture with G_3 (7mM) and PDHA (2 equiv.) before reduction ($t_{\text{red.}} = 0$). PB (3 equiv.) was added to the reaction mixture and the spectrum obtained after 120 h is shown with annotation of the resonances from the secondary amine characteristic of the reduced conjugate.

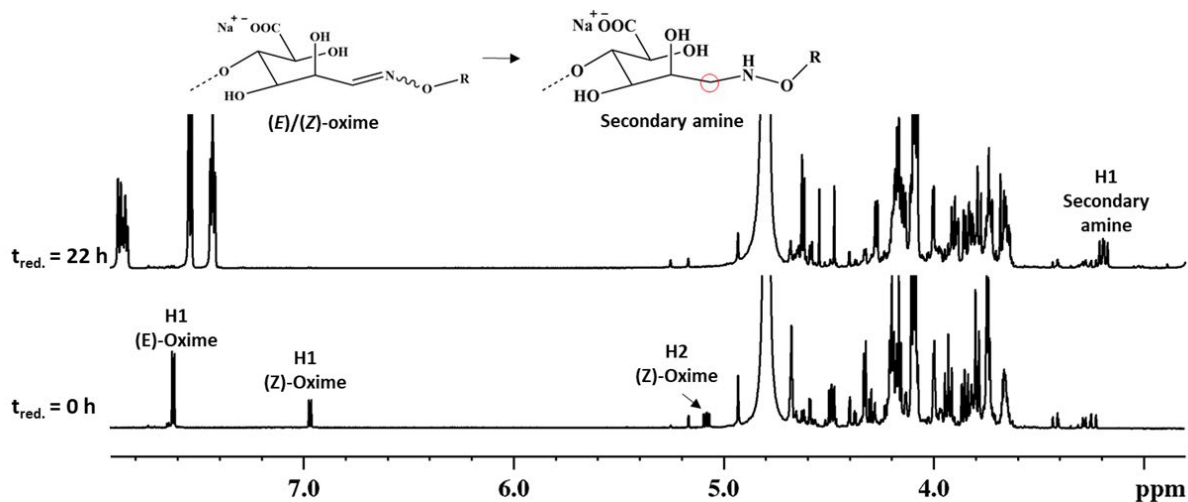


Fig. S26 ^1H -NMR (27 °C, 600 MHz) spectra of equilibrium reaction mixture with M_3 (7mM) and PDHA (2 equiv.) before reduction ($t_{\text{red.}} = 0$). PB (3 equiv.) was added to the reaction mixture and the spectrum obtained after 22 h is shown with annotation of key resonances.

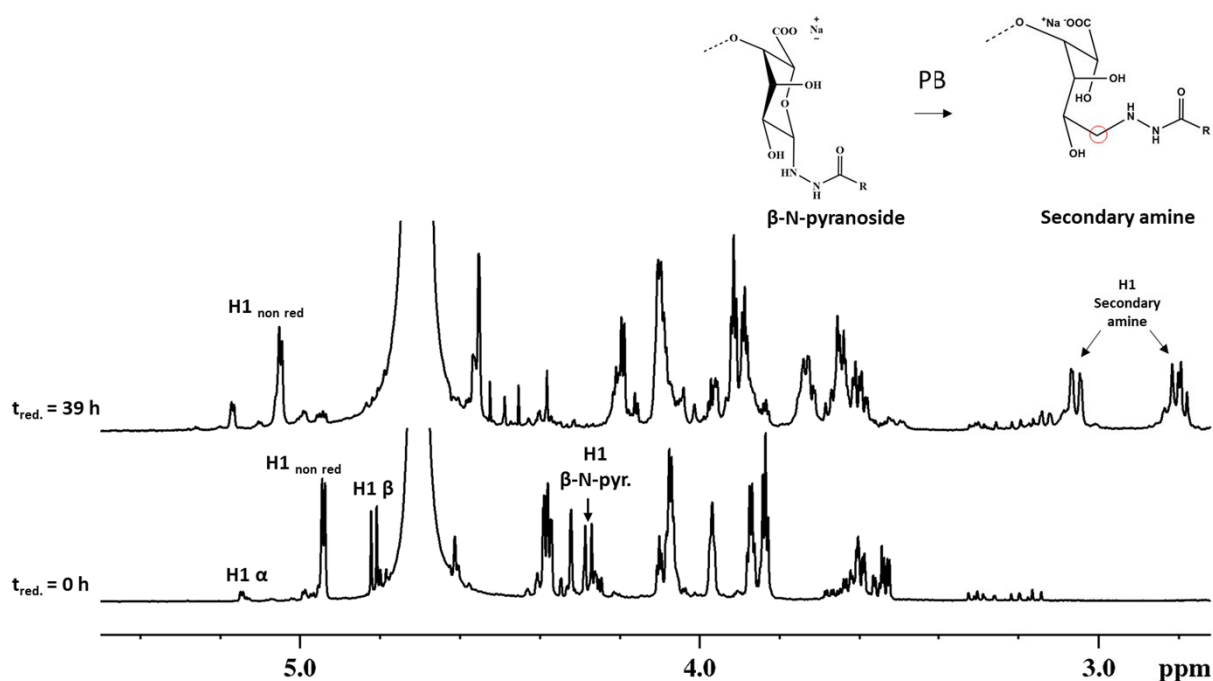


Fig. S27 ^1H -NMR (27 °C, 600 MHz) spectra of equilibrium reaction mixture with G_2 (7mM) and ADH (2 equiv.) before reduction ($t_{\text{red}} = 0$). PB (3 equiv.) was added to the reaction mixture and the spectrum obtained after 39 h is shown with annotation of key resonances.

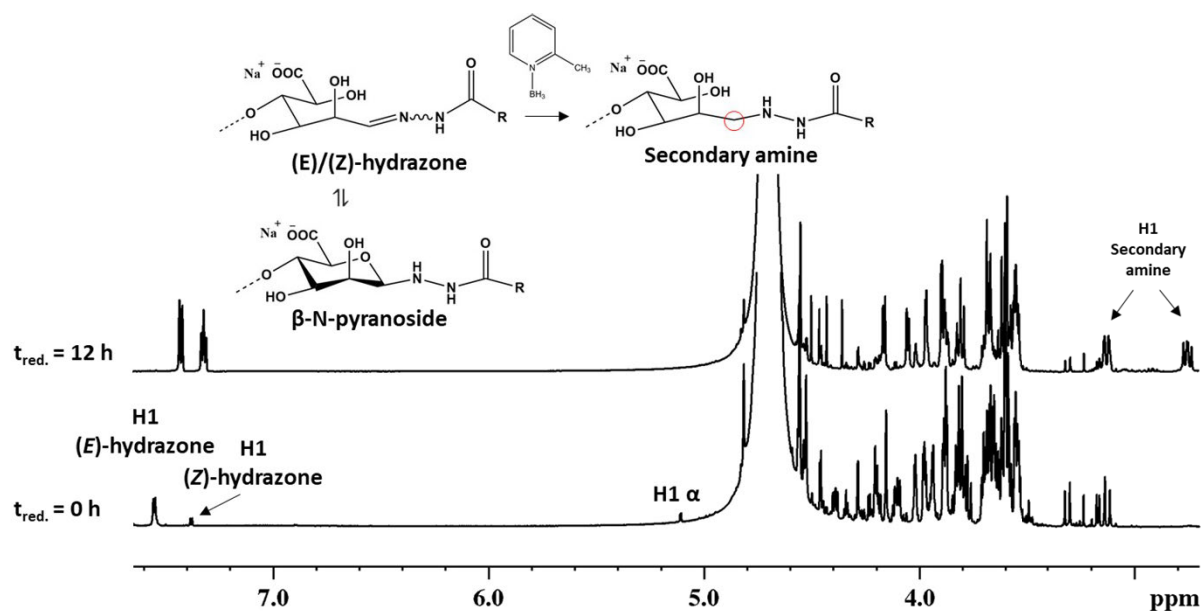


Fig. S28 ^1H -NMR (27 °C, 600 MHz) spectra of equilibrium reaction mixture with M_3 (7mM) and ADH (10 equiv.) before reduction ($t_{\text{red}} = 0$). PB (3 equiv.) was added to the reaction mixture and the spectrum obtained after 12 h is shown with annotation of key resonances.

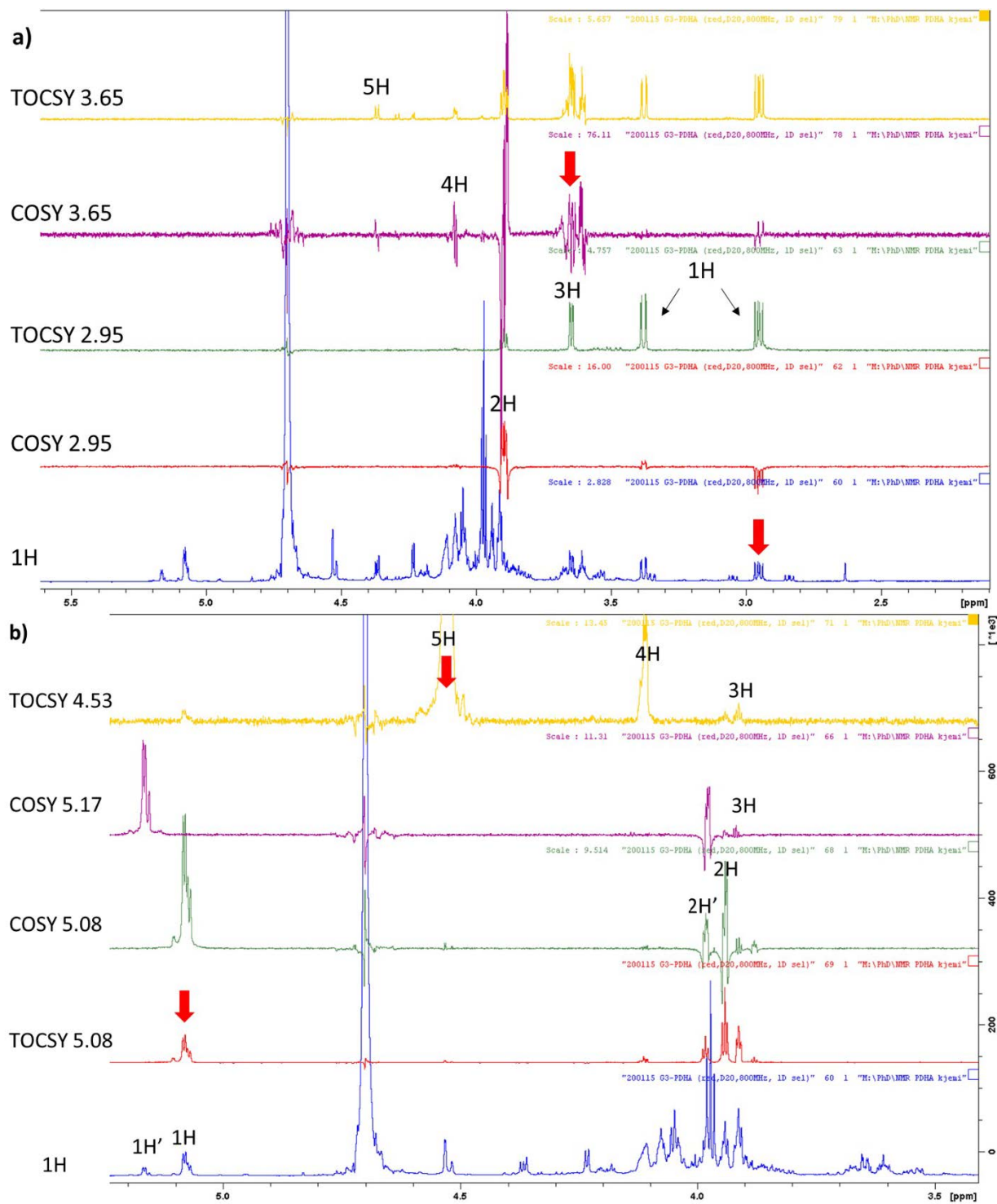
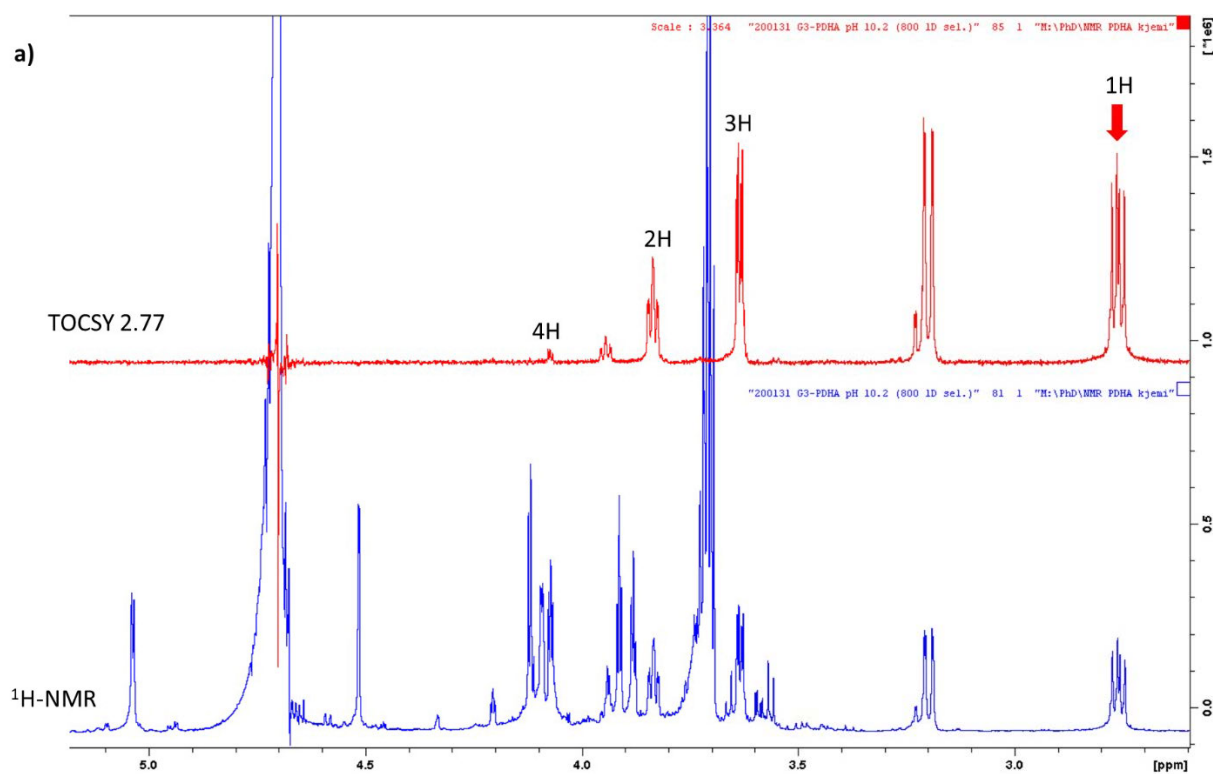


Fig. S29 Assignment of key reducing end resonances from the oxyamine modified reducing end of G₂-PDHA (with reduction, after purification by GFC, dialysis and freeze drying) in D₂O at pH 5.1 (25 °C,

800 MHz) using 1D selective COSY and TOCSY NMR. Red arrows indicate the ppm of the pulse.

Table S3: Assignment of proton resonances of G₂-PDHA (with reduction, purified by GFC, dialysis and freeze drying). Dissolved in D₂O, pH 5.1 by 1D selective COSY and TOCSY. RT is the modified reducing termini of G2-PDHA.

	H1	H2	H3	H4	H5
RT pH 5.1	2.96/3.38	3.90	3.65	4.08	4.37
	H1/H1'	H2/H2'			
NRT pH 5.1	5.08/5.17	3.94/3.98	3.92	4.11	4.53



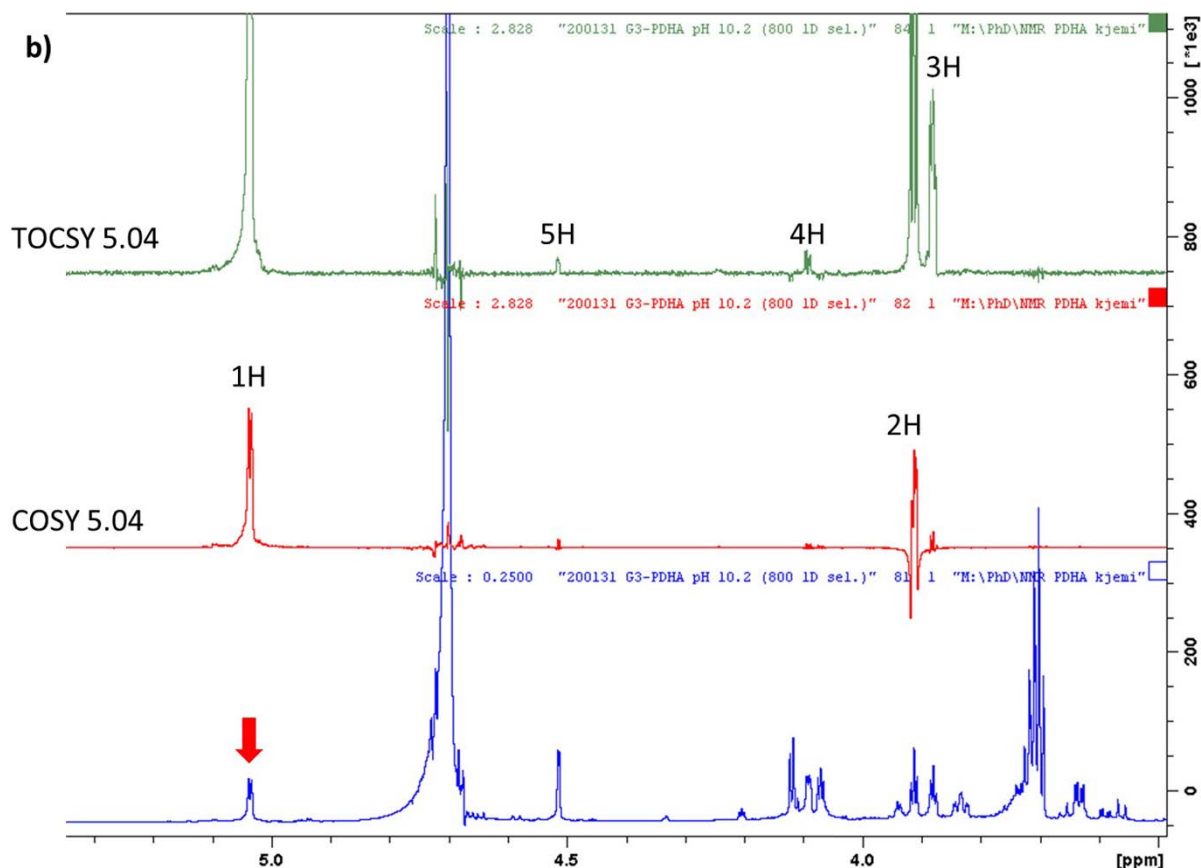


Fig. S30 Assignment of key reducing end resonances from the oxyamine modified reducing end of G₂-PDHA (with reduction, after purification by GFC, dialysis and freeze drying) in D₂O at pH 10.2 (25 °C, 800 MHz) using 1D selective COSY and TOCSY NMR. Red arrows indicate the ppm of the pulse.

Table S4: Assignment of proton resonances of G₂-PDHA (with reduction, purified by GFC, dialysis and freeze drying. Dissolved in D₂O, pH 5.1) by 1D selective COSY and TOCSY. RE denotes is the oxyamine modified reducing end of G₂-PDHA. N.d. denotes not determined.

	H1	H2	H3	H4	H5
RE pH 10.2	3.20/2.76	3.84	3.63	4.07	n.d.
NRT pH 10.2	5.04	3.91	3.88	4.09	4.52

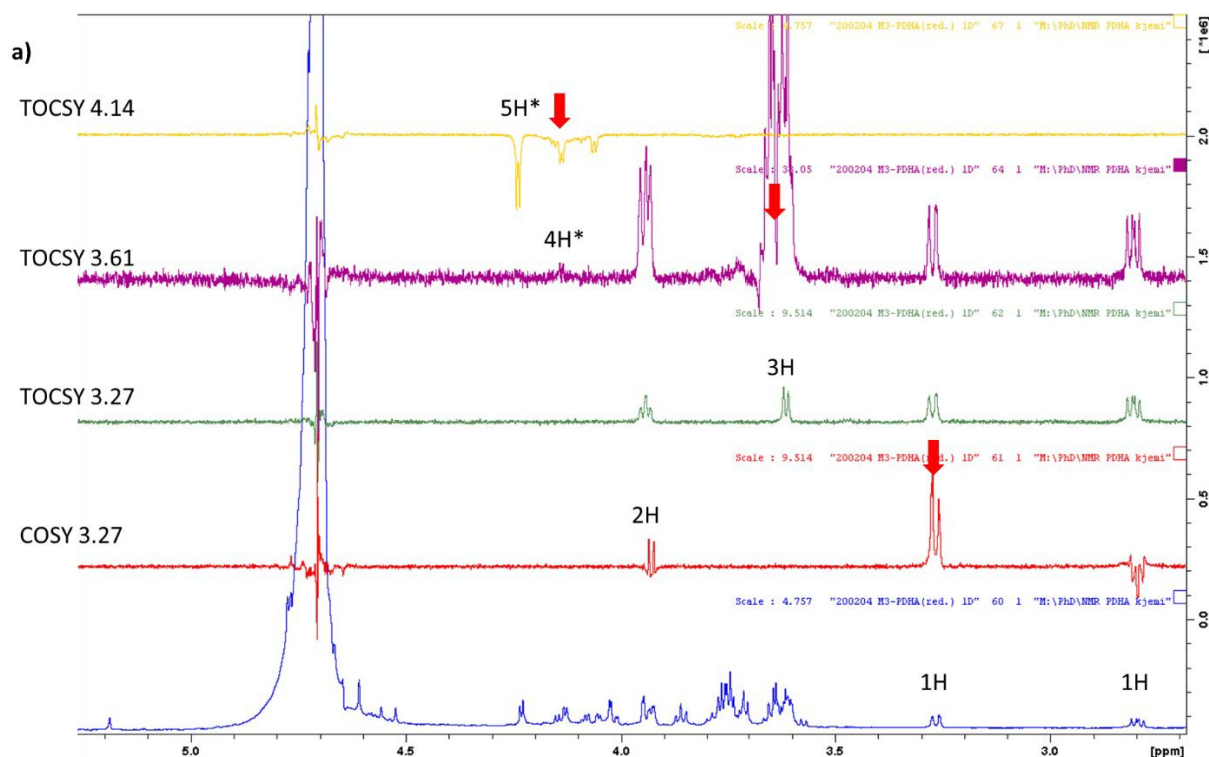


Fig. S31 Assignment of key reducing end resonances from the oxyamine modified reducing end of M₃-PDHA (with reduction, after purification by GFC, dialysis and freeze drying) in D₂O at pH 10.2 (25°C, 800 MHz) using 1D selective COSY and TOCSY NMR. Red arrows indicate the ppm of the pulse.

Table S5: Assignment of the modified reducing end (RE) of M₃-PDHA (with reduction, after purification by GFC, dialysis and freeze drying) in D₂O at pH 10.2 (800 MHz) using 1D selective COSY and TOCSY NMR. *Weak magnetization transfer

	H1	H2	H3	H4	H5
RE pH 10.7	2.80/3.27	3.93	3.61	4.14*	n.d.

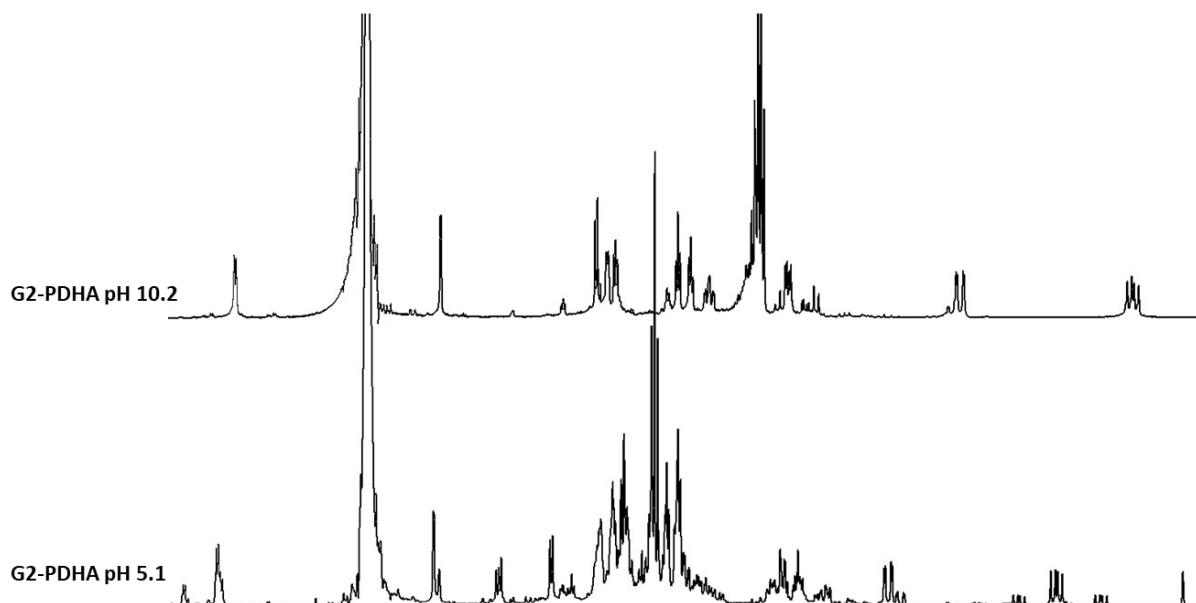


Fig. S32 ^1H -NMR (27 °C, 600 MHz) spectra of G_2 -PDHA after purification by GFC and dialysis. The sample was dissolved in D_2O and pH was adjusted from 5.1 to 10.2 with NaOD .

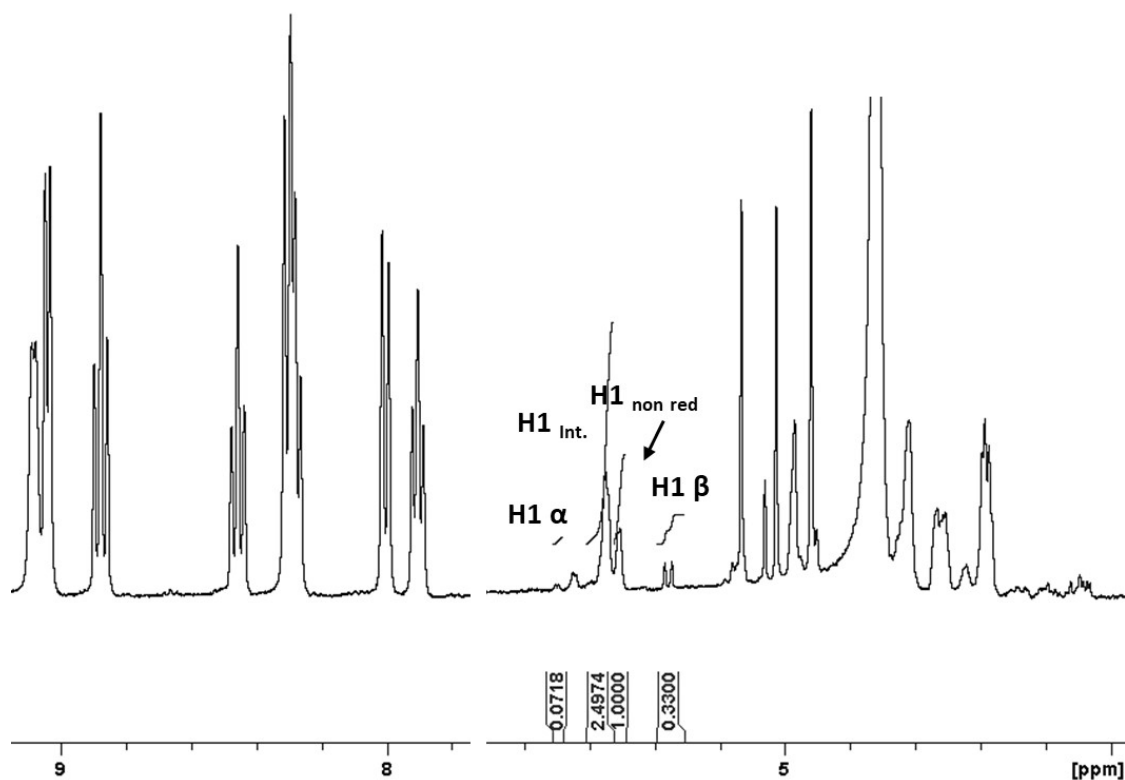


Fig. S33 ^1H -NMR spectra of G_6 (20.1 mM) with PB (20 equiv.) in 500 mM AcOHd_4 pD 4 at incubated in water bath at 40°C, recorded after 24 h (82°C, 400 MHz).

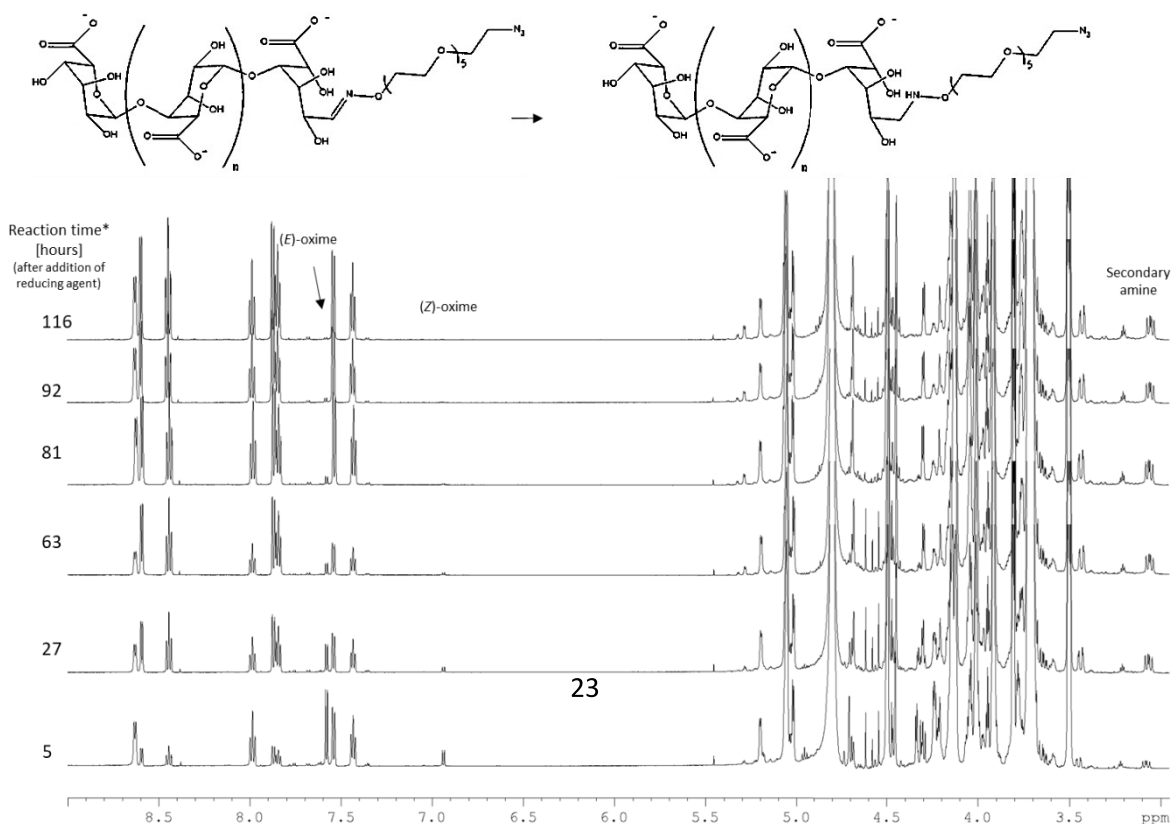


Fig. S34 $^1\text{H-NMR}$ (27 °C, 600 MHz) spectra of the reduction of the equilibrium rx. mixture with G7 (20.1 mM) and amino-ox-PEG₅-N₃ after addition of PB (3 equiv. added at t₀, another 3 equiv. added after 72 h).

Alginate-based diblock polysaccharides

A symmetrical diblock was prepared with G₁₀ and PDHA (using 0.5 equiv.) and by reduction with PB. Excess PB was removed by dialysis and the sample was freeze dried. The reaction mixture was analysed by SEC-MALS (the sample was not purified by GFC) with an in-line viscosity detector.

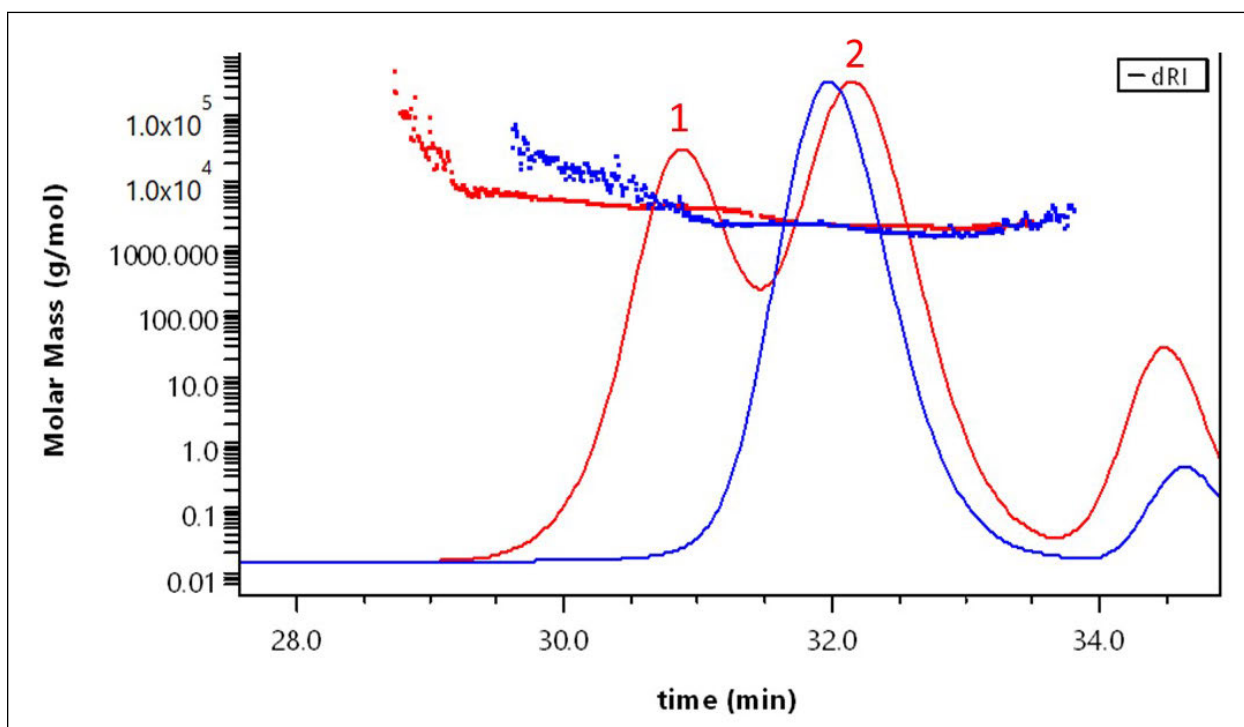


Fig. S35 A symmetrical G₁₀ was reacted with 0.5 equivalents PDHA, and the reaction mixture was analysed by SEC-MALS (red). A G₁₀ was included for comparison (blue). The coupling to form a diblock (G₁₀-PDHA-G₁₀) is manifested by a significant shift in elution volume (peak 1). Unreacted G₁₀ and G₁₀-PDHA comprise approximately 50 – 60 % of the sample (peak 2), and elutes close to pure G₁₀. Data are summarized in table S6.

Table S6: Molar mass averages of a G₁₀-b-G₁₀ block (prepared by reacting G₁₀ with 0.5 equiv. PDHA with reduction by PB, without purification by GFC) and the starting material (G₁₀). G₂₃ is included for comparison of intrinsic viscosities (see text). The data were obtained from SEC-MALS with an in-line viscosity detector, the plot of molar mass vs. time is shown in Fig. S35.

Sample	M _n (kDa)	M _w (kDa)	DP _n	[η] _w (mL/g)
G ₁₀	2.0	2.0	10	6.7

G ₁₀ -PDHA-G ₁₀ (peak 1, Fig. S35)	4.1	4.2	20	10.1
G ₁₀ (peak 2, Fig. S35)	2.1	2.2	10	6.7

References

1. Heyraud, A.; Gey, C.; Leonard, C.; Rochas, C.; Girond, S.; Kloareg, B., NMR spectroscopy analysis of oligoguluronates and oligomannuronates prepared by acid or enzymatic hydrolysis of homopolymeric blocks of alginic acid. Application to the determination of the substrate specificity of *Haliotis tuberculata* alginate lyase. *Carbohydrate Research* **1996**, *289*, 11-23.
2. Baudendistel, O. R.; Wieland, D. E.; Schmidt, M. S.; Wittmann, V., Real-Time NMR Studies of Oxamine Ligations of Reducing Carbohydrates under Equilibrium Conditions. *Chemistry* **2016**, *22* (48), 17359-17365.
3. Mo, I. V.; Feng, Y.; Dalheim, M. Ø.; Solberg, A.; Aachmann, F. L.; Schatz, C.; Christensen, B. E., Activation of enzymatically produced chitooligosaccharides by dioxyamines and dihydrazides. *Carbohydrate Polymers* **2020**, *232*, 115748.